AIMS Mathematics, 11(1): 2481–2526.
DOI: 10.3934/math.2026101
Received: 31 October 2025
Revised: 20 January 2026
Accepted: 21 January 2026
Published: 26 January 2026

https://www.aimspress.com/journal/Math

Research article

Risk aversion, safe-haven assets, and Bitcoin's evolving role in global financial markets: Insights from quantile spillover analysis

Seung Ho Choi[1], **Hayoung Choi**[1,2] **and Sun-Yong Choi**[3,*]

[1] Department of Mathematics, Kyungpook National University, Daegu 41566, Republic of Korea

[2] Nonlinear Dynamics & Mathematical Application Center, Kyungpook National University, Daegu 41566, Republic of Korea

[3] Department of Finance and Big Data, Gachon University, Seongnam 13120, Republic of Korea

* **Correspondence:** Email: sunyongchoi@gachon.ac.kr.

Abstract: In this study, we used a rolling-window quantile vector autoregression (QVAR) spillover framework to analyze how shocks associated with investor risk aversion propagate across major asset classes under different market states. The study spanned July 2014 to July 2024 and included gold, silver, Bitcoin, crude oil, major currencies, real estate investment trusts (REITs), U.S. Treasuries, dividend-paying equities, and broad equity indices. By estimating spillovers at the 10th, 50th, and 90th conditional return quantiles, we distinguished risk transmitters and risk absorbers in stressed, normal, and euphoric regimes. We then tested robustness across forecast horizons and alternative fear measures (our baseline risk-aversion index versus the VIX). The results indicated that, under normal conditions, Bitcoin is a dominant net transmitter of shocks, exporting risk to other assets, while traditional safe-haven assets, such as gold and silver, primarily absorb risk. In bull markets, Bitcoin's transmitting role intensifies and aligns with other high-beta assets, such as REITs, suggesting that Bitcoin amplifies risk-taking during periods of market optimism. However, under bear markets, Bitcoin's spillover power weakens sharply. Instead, U.S. Treasuries and gold emerge as key shock absorbers, reinforcing their defensive status during crisis periods. These findings suggest that Bitcoin is valuable for upside-oriented diversification but remains less reliable than Treasuries or gold as a downside hedge. The consistency of these patterns across horizons and fear proxies highlights the broader applicability of our framework for studying systemic risk, portfolio allocation, and safe-haven behavior.

Keywords: risk aversion; safe-haven asset; Bitcoin; QVAR spillover; bear/bull market
Mathematics Subject Classification: 62P20, 91G70

1. Introduction

Risk aversion in financial markets reflects psychological and economic forces, shaping investors' preference for low-risk assets to limit potential losses, often at the expense of higher returns. This behavior varies across market conditions and individual risk preferences. Traders in foreign exchange markets commonly adopt safety-first strategies during periods of heightened uncertainty to reduce insolvency risk [1]. Similarly, equity pricing models show that unexpected changes in profitability, interest rates, and inflation affect stock returns through shifts in investors' risk aversion [2]. Investors' heterogeneous preferences imply asymmetric attitudes toward losses and gains, potentially generating risk premiums in markets with limited downside risk and strong upside potential [3]. Accordingly, we classify market conditions using quantiles, lower, median, and upper quantiles corresponding to downturns, normal states, and booms, respectively, to examine how risk aversion relates to safe-haven assets.

Safe-haven assets are characterized by low risk and high liquidity, enabling them to store value, support short-term consumption smoothing, and serve as collateral to sustain market liquidity [4]. During periods of financial stress, such as the COVID-19 crisis and episodes of heightened geopolitical risk, assets such as gold and certain currencies function as effective hedges [5]. At the global level, widely recognized safe-haven assets can strengthen financial stability by mitigating sovereign default risk [6]. As economic uncertainty increases and alternative secure investments become scarce, investors increasingly concentrate capital in perceived safe assets [7]. Consequently, the relationship between risk aversion and safe-haven assets has been extensively examined across diverse market regimes.

The link between risk aversion and safe-haven assets becomes especially pronounced during periods of market turbulence. Assets such as gold and major safe-haven currencies tend to preserve or increase their value amid heightened volatility, making them attractive to risk-averse investors. Because asset returns are constructed from U.S. dollar-denominated price series, the U.S. dollar serves as the numéraire and is therefore not included as a standalone return series. Instead, we incorporate major exchange rates quoted against the U.S. dollar to capture currency safe-haven dynamics in a consistent measurement framework [8]. While not all assets qualify as safe havens, global shifts in risk aversion are often reflected in the returns of recognized safe-haven assets [9]. However, strong performance during periods of crisis highlights the trade-off between protection in stress episodes and relatively lower returns during tranquil periods. Consequently, rising risk aversion prompts investors to reallocate capital toward assets such as gold and U.S. Treasury bonds [10]. The effectiveness of safe-haven assets also differs markedly across advanced and emerging markets and during systemic crises [11]. Accordingly, we analyze the relationship between selected safe-haven asset candidates and risk aversion across market regimes and over time.

Despite the growing literature on risk aversion and safe-haven assets, several important gaps remain. First, much of the research relies on mean-based econometric frameworks, which obscure heterogeneity across the return distribution and fail to capture asymmetric behavior during extreme market conditions. Second, researchers typically focus on a narrow set of assets or specific crisis episodes, limiting the ability to draw general conclusions about how risk aversion propagates through a broader financial network. Third, although Bitcoin has attracted significant academic and investor attention, its role as a transmitter or absorber of risk relative to traditional safe-haven assets has not

been systematically examined across market states.

Or primary motivation of this study is to address these gaps by developing a unified, distribution-sensitive framework that explicitly links global risk aversion to a broad set of safe-haven asset candidates under different market regimes. To this end, we adopts a unified framework that enables a comprehensive examination of the relationship between global risk aversion and safe-haven asset candidates across market states. In particular, we analyzes changes in safe-haven asset prices in relation to different levels of risk aversion and investigate the dynamic relationships between these variables. Methodologically, we employ a rolling-window quantile vector autoregression (QVAR)–based spillover framework to capture the impact of risk aversion on safe-haven assets across the conditional distribution of returns. By analyzing relationships at various quantiles, this approach enables us to differentiate asset behavior under normal market conditions from that observed during periods of extreme stress or exuberance. Moreover, spillover measures are incorporated to quantify how shocks propagate between variables across horizons and quantiles. Our study enhances the understanding of the nonlinear and state-dependent dynamics between global risk aversion and safe-haven assets and provides a more nuanced toolkit for researchers and practitioners to identify and manage risk across market conditions. Notably, the QVAR-based spillover framework has been increasingly applied in financial research due to its ability to capture asymmetric and state-dependent interdependencies across assets [12–18].

An additional motivation for adopting a nonlinear modeling framework is the growing empirical evidence that spillovers in financial markets are state-dependent and asymmetric. Studies have shown that linear, mean-based models often fail to capture heterogeneous shock transmission, particularly during periods of extreme market stress. For example, spillovers between precious metals and oil vary substantially across quantiles, with tail-risk transmission dominating during turbulent periods [19]. Similarly, sectoral and real estate market analyses document strongly nonlinear and regime-dependent responses to downturns and monetary policy shocks [20, 21]. Motivated by this literature, we employ a rolling-window QVAR-based spillover framework to capture the asymmetric and state-dependent transmission of risk aversion across traditional and emerging safe-haven assets.

In this study, we employ the risk-aversion index (RAI) introduced by the researchers in [22]. This index captures variations in global risk aversion by quantifying the degree to which investors require additional compensation for holding riskier assets. A higher index value indicates a stronger preference for safer investments. Additionally, we incorporate several well-established safe-haven assets to investigate their dynamic relationship with the degree of risk aversion, as measured by the risk aversion index. A detailed review of the risk aversion index and selected safe-haven assets is provided in the following section.

We investigate how the connectedness between risk aversion and safe-haven assets evolves over time and capture these dynamic relationships across market conditions (quantiles) using a rolling-window QVAR-based spillover framework. This approach assumes homogeneity in spillover effects at the center of the distribution while enabling heterogeneity in the tails. It enables us to assess how the strengths and directions of spillover effects between the RAI and safe-haven assets differ under normal market conditions (middle quantiles) and extreme market movements (tails). A detailed explanation of the methodology is provided in the section *QVAR-Based Spillover Framework*.

This study makes several contributions to the literature. First, by incorporating an RAI, we directly measure the degree of market participants' risk aversion and examine its linkage with safe-haven assets.

Second, we empoly a rolling-window QVAR-based spillover framework to analyze the interactions between traditional and emerging safe-haven assets and a direct, model-based measure of global risk aversion. This approach captures state-dependent and time-varying spillover dynamics across bear, normal, and bull market regimes. Rather than proposing a new econometric model, we demonstrates how an established quantile-based spillover methodology can be systematically applied to examine distribution-dependent dynamics and asymmetric shock transmission. The empirical analysis serves as an illustrative application, highlighting the framework's ability to capture tail-dependent and regime-specific interactions, with particular emphasis on Bitcoin's evolving role relative to traditional safe-haven assets.

Research has shown that connectedness and spillover transmission mechanisms are strongly state-dependent and may differ substantially across quantiles (and, in some applications, across frequencies), meaning that mean-based VAR connectedness can mask tail-specific propagation patterns. Quantile connectedness approaches have been applied to monetary policy transmission channels (e.g., interest-rate swap markets) and to sustainable, green, and clean-energy related asset systems, documenting pronounced asymmetries across distributional states [23, 24]. Similar quantile dependence has also been observed in cryptocurrency and commodity-related networks, where tail regimes exhibit stronger and more asymmetric connectedness, and the identity of net transmitters and receivers may switch across quantiles [19, 25, 26]. Motivated by this literature, we interpret our QVAR-based connectedness estimates as a risk-aversion-driven propagation mechanism that can vary across stress (lower tail), normal (median), and exuberant (upper tail) regimes within a broad multi-asset safe-haven system.

Furthermore, we conduct robustness checks by varying the forecast horizon and find that the spillover estimates remain stable across horizons, confirming the reliability of our results. Additionally, we compare the baseline (RAI) with the VIX as an alternative proxy. The consistent spillover patterns observed across both measures highlight the robustness of our findings and demonstrate the broader applicability of our framework in capturing market fear and uncertainty.

We further enhance its practical relevance by including an analysis of Bitcoin, one of the most closely watched assets in recent financial markets and academic research. By incorporating Bitcoin into the empirical framework, this study provides insights that are academically meaningful and directly applicable to current market dynamics.

The remainder of this paper is structured as follows. In the next section, we review the relevant literature. In the *data* section, we introduce the RAI and the selected safe-haven assets. In the *QVAR-Based Spillover Framework* section, we provide a brief overview of the QVAR-based spillover methodology employed in this study. In the *Spillover Analysis: Results and Discussion* section, we present and interpret the empirical findings. Finally, in the *Concluding Remarks* section, we outline this study's key implications and contributions.

2. Literature review

In this section, we begin by reviewing studies on the RAI. Specifically, we first discuss key research that entails the RAI introduced in the previous section. Subsequently, we examine studies that use the VIX as a proxy for risk aversion. Consistent with this study's objectives, we also review the literature on the relationship between safe-haven assets and financial markets. Furthermore, we highlight several studies that investigate Bitcoin's potential role as a safe-haven asset.

Recent cryptocurrency literature supports the view that cross-market linkages are strongly state-dependent. Using high-frequency data and a GMM-based regime classification, Joshi (2025) reported that interdependencies intensify in volatile regimes, with Bitcoin frequently acting as a shock transmitter [27]. Ko and Chen (2025) further documented pronounced time–frequency co-movements between Bitcoin and AI-related tokens, arguing that Bitcoin provides limited hedging benefits against these tokens across horizons [28]. These findings complement our quantile-regime interpretation (bear, normal, bull) and provide external support explaining why Bitcoin tends to align with risk-on assets in bull regimes within our multi-asset connectedness system.

2.1. Risk aversion index

The RAI has been widely used in financial research, with studies demonstrating its explanatory power across asset classes and market conditions. The researchers in [22] developed a daily RAI constructed from six market indicators, showing that, when embedded in the stochastic discount factor, it captures a large portion of equity and corporate bond excess returns, along with risk-neutral equity volatility. Building on this foundation, the researchers in [29] employed the index as a global uncertainty factor in analyzing the connectedness between real estate tokens, real estate investment trusts (REITs), gold, and Bitcoin. Their results revealed that heightened risk aversion during bear markets amplifies spillover effects across these assets, increasing total connectedness. Further extending its applications, the researchers in [30] incorporated the index into an extended Heterogeneous Autoregressive (HAR) model to improve volatility forecasts and cross-market correlation predictions. Their approach not only enhances predictive accuracy but also delivers greater economic value, leading to lower portfolio risk compared to competing models. The index also serves as a real-time barometer of market stress, as evidenced by the researchers in [31], who documented a sharp spike in risk aversion during the March 2020 COVID-19 crash, reinforcing their experimental findings that financial professionals become significantly more risk-averse when aggregate market uncertainty rises.

In addition to direct RAIs, alternative measures such as the VIX have been widely used in the literature to capture market risk aversion. The researchers in [32] employed three distinct RAIs, the Global Risk Aversion Index (GRAI), a principal component analysis (PCA)-based index, and the VIX, to estimate crisis probabilities across 20 foreign exchange and equity markets. Using logit and multinomial logit models, they demonstrated that these indices serve as reliable leading indicators of financial stress. Further refining the interpretation of the VIX, the researchers in [33] decomposed it into separate risk aversion and uncertainty components. Their findings revealed that expansionary monetary policy has a stronger dampening effect on risk aversion than on uncertainty, with the impact becoming statistically significant after approximately nine months.

2.2. Safe-haven assets and the financial market

Safe assets underpin economic stability by serving as stores of value and collateral, thereby smoothing consumption and supporting credit. The interaction between public and private safe assets shapes their supply and perceived safety. These dynamics influence the broader economic performance and efficiency of financial markets [4]. Similarly, the researchers in [5] examined the safe-haven properties of gold, Bitcoin, and major currencies during major global events from 2014 to 2022,

including the COVID-19 pandemic and Russia's invasion of Ukraine. They found that the Japanese yen is the strongest safe-haven asset, whereas Bitcoin is a weak safe-haven asset that shows no negative correlation with stock indices over the period. The researchers in [6] argued that addressing the combined challenges of sovereign default risk and safe-asset scarcity is critical for global financial stability, underscoring the importance of understanding how safe assets function and how defaults constrain their supply. Such insights can inform the design of international financial institutions aimed at stabilizing the financial system and maintaining a steady global supply of safe assets. According to [7], an asset's safety is a coordination outcome rooted in investors' shared beliefs. When few substitute safe assets are available, these beliefs concentrate demand and, in turn, reinforce the asset's perceived and realized safety.

Researchers have examined Bitcoin's potential as a safe-haven asset. The researchers in [34] employed a bivariate cross-quantilogram approach to compare Bitcoin with gold and commodities across global equity markets, revealing divergent safe-haven properties. Bitcoin demonstrates moderate effectiveness in emerging markets (e.g., China) but exhibits limited and inconsistent performance in developed economies, suggesting that it functions as a weak and market-dependent safe haven. The researchers in [35] critiqued Bitcoin's practical viability through a comparative analysis of volatility, liquidity, and transaction costs, highlighting structural limitations, including excessive price fluctuations, illiquidity, and high trading fees, that undermine its reliability relative to traditional hedges, such as gold. These findings imply that Bitcoin market maturation is a prerequisite for its adoption as a stable safe haven. Complementing these insights, The researchers in [36] utilized wavelet quantile and Granger causality methods to demonstrate Bitcoin's asymmetric responsiveness to U.S. uncertainty shocks; while it intermittently functions as a hedge during periods of heightened turmoil, its efficacy is highly sensitive to time horizons and prevailing market regimes. Collectively, these studies underscore that Bitcoin's safe-haven attributes are conditional and non-uniform, warranting cautious interpretation by investors and researchers alike.

2.3. Risk aversion and safe-haven assets

Researchers investigating the link between risk-averse behavior and safe-haven assets have shown that Bitcoin exhibits limited safe-haven properties, particularly during extreme market downturns in Chinese and Asia-Pacific stocks [37]. Despite its appeal to risk-averse investors in these regions, Bitcoin's broader safe-haven characteristics are constrained by high volatility, low liquidity, and transaction costs relative to gold [35]. Although Bitcoin, gold, and other commodities provide weak safe-haven protection against global stock indices, Bitcoin's role is highly time- and region-dependent. It serves as a safe-haven asset in crisis-stricken Venezuela, a diversifier in Japan and China, and a weak hedge in Sweden and Estonia [38]. Its safe-haven appeal is more prominent in Chinese markets than in developed ones [34]. Wavelet analysis suggests that Bitcoin offers better diversification benefits and safe-haven properties than gold and other commodities during extreme downturns [39]. However, gold consistently serves as a reliable safe-haven asset across G7 markets, whereas Bitcoin's effectiveness is weaker and varies by region, as seen in Canada and France [40]. In the U.S., Bitcoin's safe-haven role fluctuates during periods of political and economic uncertainty and is influenced by events such as elections, COVID-19, and policy shifts [36]. Furthermore, global risk aversion predicts safe-haven asset returns, with silver and oil exhibiting consistent safe-haven properties, whereas Bitcoin and gold show time-varying behaviors shaped by market and investor dynamics [9].

Although the literature provides valuable insights into risk aversion, safe-haven assets, and their interactions, several important gaps remain. First, most empirical studies rely on mean-based or linear frameworks that implicitly assume homogeneous responses across market conditions. Such approaches are ill-suited to capturing the asymmetric and nonlinear dynamics that emerge during extreme market states, particularly in the tails of the return distribution, where risk aversion is most pronounced.

Second, researchers typically focus on a limited subset of assets or specific crisis episodes, thereby restricting the ability to generalize findings across asset classes and market regimes. While individual studies examine gold, currencies, or Bitcoin in isolation, relatively few adopt a unified framework that simultaneously evaluates traditional safe-haven assets, cryptocurrencies, equities, bonds, and real estate securities within a single interconnected system.

Third, the literature on Bitcoin's safe-haven role remains inconclusive. Evidence suggests that Bitcoin's hedging properties are highly time-varying and regime-dependent; however, most researchers do not explicitly distinguish downside, normal, and upside market conditions when assessing its spillover behavior relative to conventional safe-haven assets.

In this study, we directly address these gaps by employing a rolling-window QVAR–based spillover framework that enables spillover effects to vary across market states and over time. By examining connectedness at multiple conditional quantiles, we capture tail-specific and regime-dependent transmission mechanisms overlooked in mean-based analyses. Moreover, by incorporating a broad set of asset classes alongside a model-based RAI and alternative fear proxies, our framework provides a comprehensive assessment of how global risk aversion propagates through financial markets and clarifies Bitcoin's evolving role relative to established safe-haven assets.

2.4. Hypothesis development

The empirical literature suggests that the relationship between risk aversion and financial assets is inherently nonlinear and state dependent. During periods of elevated uncertainty, investors rebalance portfolios toward assets perceived as safe, whereas during normal or euphoric market conditions, riskier assets tend to dominate capital flows. However, these dynamics are not uniform across assets or market regimes, motivating the formulation of testable hypotheses that reflect asymmetric spillover behavior.

Researchers have documented that traditional safe-haven assets, such as gold and U.S. Treasuries, tend to absorb shocks during market downturns, thereby acting as net receivers of risk when investor risk aversion rises [7, 10, 41].

Conversely, during stable or bullish periods, these assets play a more passive role as investors shift toward higher-yielding alternatives. This leads to the first hypothesis:

H1: *Traditional safe-haven assets (e.g., gold and U.S. Treasuries) act as net receivers of risk-aversion spillovers during bearish market conditions, while their spillover influence weakens under normal and bullish regimes.*

The literature further indicates that spillover dynamics intensify during extreme market conditions. Researchers employing quantile-based or tail-focused approaches show that connectedness across assets is substantially stronger in the lower and upper tails of the return distribution than around the mean [42, 43]. This suggests that risk transmission mechanisms are asymmetric and regime-specific:

H2: *Total and directional spillovers associated with risk aversion are significantly stronger in the tails of the return distribution (bear and bull markets) than in the median state.*

Finally, empirical evidence on Bitcoin's role as a safe-haven asset remains mixed. While some researchers document hedging or diversification benefits under specific conditions, others find that Bitcoin behaves more like a speculative, high-risk asset, particularly during periods of market stress [34, 37, 44]. Studies also suggest that Bitcoin may transmit rather than absorb shocks during periods of heightened risk-taking, raising questions about its reliability as a downside hedge:

H3: *Bitcoin acts primarily as a net transmitter of risk-aversion spillovers during normal and bullish market conditions, while its spillover influence weakens during bearish regimes relative to traditional safe-haven assets.*

These hypotheses are empirically tested using a rolling-window QVAR-based spillover framework that enables spillover effects to vary across market states and over time. By jointly examining multiple asset classes and conditional quantiles, the analysis directly evaluates how risk-aversion shocks propagate through financial markets under different regimes.

3. Data

3.1. Risk aversion index

We employ the RAI introduced by the researchers in [22], which integrates financial market data such as stocks, bonds, derivatives, implied volatility, and market-sentiment indicators. Unlike static measures of risk aversion, this index captures time-varying changes, facilitating a more nuanced analysis of investor behavior across economic cycles. This index has been widely used in financial research [30, 45–49]. The RAI is obtained from the authors' website*.

The RAI offers a dynamic, model-based measure of investors' risk preferences over time (see Figure 1). In contrast to conventional approaches that assume constant risk aversion, the RAI aggregates macroeconomic and market-based inputs, such as return variances, credit spreads, and option-implied indicators, including the VIX, to track fluctuations in economy-wide risk appetite, particularly during periods of market stress [22].

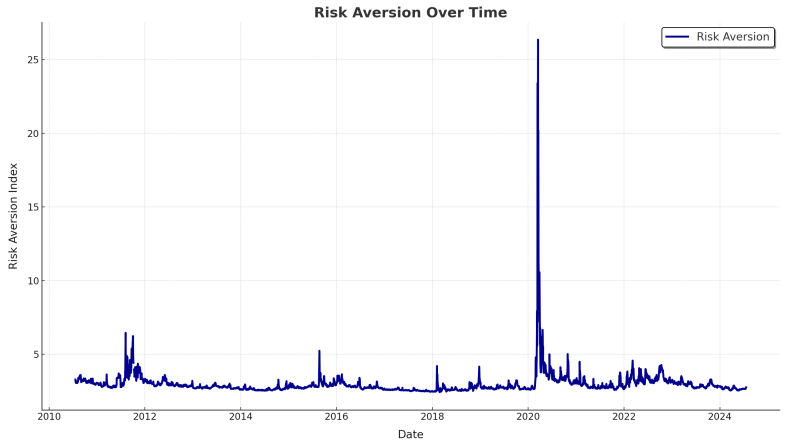

Figure 1. Risk-Aversion Index from 2014 to 2024. This figure plots the RAI used in the multivariate system. Higher values indicate higher aggregate risk aversion (lower risk appetite), which is expected to coincide with heightened market stress.

*https://www.nancyxu.net/risk-aversion-index

3.2. Safe-haven assets

Daily market price data are downloaded from Yahoo Finance using the `yfinance` Python package (`https://pypi.org/project/yfinance/`) and converted into USD-denominated returns. The risk-aversion index (raBEX/RABEX) is obtained from Nancy Xu's Risk Aversion Index data page (`https://www.nancyxu.net/risk-aversion-index`). A detailed description of each asset, including its full name and abbreviation, is provided in the Appendix Table A.1.

We collect and analyze 18 variables, along with risk aversion, from July 1, 2014, to July 14, 2024, to examine their interconnectedness and underlying dynamics (see Table A.1). The selected variables span a diverse range of asset classes, including traditional safe-haven assets (e.g., gold and U.S. Treasuries), precious metals and commodities (e.g., silver and crude oil), national equity market indices, currencies, digital assets (e.g., Bitcoin), dividend-paying stocks, and REITs. Incorporating this broad set of instruments enables us to capture the multifaceted nature of safe-haven behavior, hedging characteristics, and nonlinear state-dependent transmission of risk across segments of the global financial market.

Gold is a canonical safe-haven asset that responds positively to spikes in implied volatility (VIX) and provides stability during episodes of severe market stress [41,50]. Similarly, silver exhibits certain hedging characteristics attributable to its sensitivity to inflation uncertainty and geopolitical risks, although its safe-haven role diminished during the COVID-19 crisis [51, 52]. Crude oil, which is not traditionally classified as a safe-haven asset, has shown potential in stabilizing properties in specific contexts, such as when evaluated alongside clean-energy investments [53]. Moreover, commodity futures generally offer important portfolio-diversification benefits and display low correlation with conventional assets such as equities and bonds, enabling investors to mitigate portfolio risk and improve risk-adjusted returns [54]. Notably, speculative activity in crude-oil futures is inversely correlated with market risk aversion, with heightened speculation (e.g., 2005–2008) associated with diminished risk aversion and lower risk premiums [55].

Regarding equity markets, certain national stock market indices and their corresponding ETFs can serve as effective hedges during the mature phases of financial crises, demonstrating capabilities akin to traditional safe-haven assets such as precious metals [56]. Although gold and silver are more suitable for hedging abrupt shocks, well-established equity benchmarks function reliably during prolonged downturns. Additionally, investing in a diversified basket of stocks, such as those comprising a national index, can reduce idiosyncratic risk and provide hedging benefits against inflation and currency depreciation in stable markets, aligning these instruments with conventional safe-haven assets [2, 57, 58]. To reflect regional differences in market sentiment and investor behavior, we include ETFs corresponding to the stock indices of Korea, the U.S., Japan, China, and Europe.

Currencies are integral to understanding the global landscape of risk aversion. The Japanese yen (JPY) consistently exhibits safe-haven attributes across major global equity indices, underscoring its role as a reliable financial refuge [5]. The internationalization of the Chinese yuan (CNY) may confer greater macroeconomic flexibility and leverage on China, suggesting its potential emergence as a safe-haven currency [59]. The British pound (GBP), while theoretically plausible as a safe-haven asset, remains contingent on broader economic conditions and investor perceptions [60], whereas the euro (EUR) has demonstrated resilience during Eurozone financial turmoil, potentially aiding more effective risk-sharing among member states [61]. Thus, foreign exchange rates serve as critical indicators of market sentiment, and heightened risk aversion often constrains speculative activities and increases

demand for safe-haven currencies, linking exchange rates directly to global risk transmission [1]. All series in our dataset are constructed from U.S.-dollar-denominated prices; hence, the U.S. dollar serves as the numéraire in our system. Accordingly, we do not include the U.S. dollar (or a dollar index) as a separate variable; instead, we use major exchange rates involving the U.S. dollar, reported in standard market conventions (EUR/USD, GBP/USD, USD/JPY, and USD/CNY), to capture currency safe-haven dynamics [8].

In addition to traditional and semi-conventional assets, emerging instruments have garnered attention. For example, Bitcoin has maintained its safe-haven status over extended periods, even as market uncertainty subsides. This suggests that Bitcoin can act as an effective refuge under specific market conditions [62]. Moreover, Bitcoin is a leading transmitter of risk-aversion spillovers within and between traditional financial markets, reflecting its integral role in capturing evolving risk preferences [44].

Dividend-paying equities are also included to investigate how high-dividend-yield companies operate under risk-averse market conditions. Researchers have linked dividend payouts to expected returns in risk-averse environments, with higher dividend yields serving as indicators of investor sentiment and underlying uncertainty [63, 64]. Companies with stable and substantial dividends attract more investor attention when risk aversion is elevated, because dividends can help moderate severe price declines and provide relatively stable returns. Hence, we incorporate Coca-Cola, Johnson & Johnson, and AT&T, which are prominently represented in dividend-focused ETFs. Coca-Cola constitutes 1.57% of the Vanguard High Dividend Yield ETF (VYM) and 2.34% of the WisdomTree U.S. Quality Dividend Growth Fund (DGRW). Johnson & Johnson accounts for 2.21% of VYM and 3.08% of DGRW, whereas AT&T represents 0.89% of VYM and 2.4% of the Global X SuperDividend U.S. ETF (DIV). Their substantial presence in ETFs reinforces their status as leading dividend-paying stocks and justifies their inclusion as representative assets.

U.S. Treasury bonds are incorporated because of their established standing as classic safe-haven securities. The sizeable U.S. debt scale and consistent market confidence in Treasuries underscore their function as benchmark assets, reflecting shifts in risk aversion through yield spreads and risk premiums [7, 65]. Finally, we include REITs to assess the role of real-estate securities in mitigating stock market volatility. The Vanguard Real Estate ETF exhibits smaller drawdowns than non-REIT equities during market downturns, suggesting partial insulation from heightened uncertainty [66]. Additionally, time-varying risk aversion is a significant predictor of regime shifts in REIT markets, enabling more effective forward-looking hedging strategies that substantially reduce portfolio risk [67].

Taken together, these carefully selected variables, ranging from traditional safe-haven assets and commodities to equities, currencies, digital assets, dividend-paying stocks, bonds, and REITs, provide a comprehensive basis for examining how changes in global risk aversion diffuse through intricate financial networks.

4. Theoretical mechanisms and testable expectations

Our empirical design is motivated by the view that aggregate risk aversion is a state variable that governs the pricing of risk and, consequently, the strength of cross-market transmission. Habit-based asset-pricing models formalize this idea by generating time variation in the effective price of risk (risk premiums) over the business cycle [68].

A risk-aversion shock can be interpreted as a tightening of financial conditions that triggers portfolio rebalancing and balance-sheet adjustments across asset classes. Importantly, this propagation mechanism is unlikely to remain constant across market states: Lower-tail regimes tend to feature binding funding and margin constraints and reduced market liquidity, whereas upper-tail regimes are associated with risk-taking and reach-for-yield behavior. These channels provide an economic rationale for employing a quantile-based system rather than a mean-based VAR. The key implication of these channels is that cross-asset transmission should *re-rank* across distributional states. In lower-tail regimes (bear markets), tighter funding liquidity and higher margin requirements can trigger liquidity spirals and forced deleveraging, which strengthen spillovers among risky assets while increasing the relative hedging demand for traditional safe havens [69, 70]. In upper-tail regimes (bull markets), risk-taking and speculative positioning can increase common-factor co-movement among high-volatility assets. In this environment, Bitcoin is often reported to behave more like a speculative asset than a stable safe haven, providing an economic rationale for its stronger alignment with high-risk assets in bull markets [35, 71, 72]. Hence, a quantile framework is not only a statistical device but also an economically interpretable way to map the system onto risk-off (lower-tail) versus risk-on (upper-tail) regimes [25, 43].

4.1. Why spillovers differ across quantiles

In bearish conditions, increased risk aversion can amplify spillovers through reinforcing channels. First, tighter funding and margin conditions reduce intermediaries' risk-bearing capacity. When funding liquidity deteriorates, market liquidity is impaired, generating liquidity spirals that lead to synchronized deleveraging and larger price dislocations across markets [69]. Second, flight-to-quality episodes can induce liquidity hoarding and a broad contraction in risk exposure, which, in turn, may increase systemic risk and create a "gridlock" environment in which shocks propagate more sharply [70]. Together, these mechanisms imply that shocks may propagate more strongly in the lower tail and that directional spillovers can intensify when many investors rebalance simultaneously.

In contrast, in bullish conditions, the dominant channel is often risk-on reallocation, where improving risk appetite encourages exposure to risky assets and can alter the magnitude and direction of spillovers relative to stressed regimes. Therefore, the same innovation to risk aversion can produce asymmetric transmission patterns across quantiles; specifically, the type of state dependence that the QVAR connectedness framework is designed to capture.

4.2. Variable selection and expected spillover patterns

The selected variables represent distinct hedging and risk-bearing channels through which risk-aversion shocks can be transmitted. Traditional safe-haven assets such as gold are expected to absorb risk during stress episodes, which is with evidence that gold can act as a safe haven during extreme stock-market downturns [41]. Major currencies and broad equity indices capture international risk transmission and global portfolio rebalancing. REITs and dividend-oriented equities represent interest-rate- and cash-flow-sensitive segments, which may respond strongly to tightening financial conditions. Commodities (e.g., crude oil) reflect macroeconomic and geopolitical risk, as well as demand-side shocks that can be amplified during tail events. Thus, digital assets (e.g., Bitcoin) are included to evaluate whether their role resembles that of a Diversifier, safe haven, or a risk asset, noting that

empirical evidence suggests Bitcoin's hedge and safe-haven properties can be market-specific and may differ across stress episodes [37].

These mechanisms imply testable expectations. In the lower tail, risk-aversion shocks are more likely to generate greater total connectedness and stronger directional spillovers due to funding constraints, liquidity spirals, and flight-to-quality dynamics. Safe-haven assets are expected to act as relative absorbers (higher FROM than TO), whereas riskier assets may act as net transmitters of distress. In the upper tail, spillovers may be driven more by risk-on reallocation, potentially altering the net spillover roles of certain assets, including Bitcoin, relative to stressed states. The empirical sections evaluate these regime-dependent predictions using quantile-specific connectedness measures.

5. The QVAR-based spillover framework

A QVAR-based spillover framework is employed to capture the dynamic interrelationships across levels of risk aversion and various quantiles of the conditional distribution. Our analysis builds on the QVAR-model-based spillover methodology proposed [43], which we implement in a rolling-window setting for a multi-asset safe-haven system that includes a model-based risk-aversion proxy as an endogenous variable. Throughout, the resulting indices are interpreted as directional spillovers (predictive shock transmission) rather than indicators of structural causality.

A QVAR model is employed to analyze the interdependencies among m variables across quantiles [43]. The data can be expressed as an $n \times m$ matrix, where n represents the number of observations. Let $Y_t \in \mathbb{R}^m$ denote the observed vector of the m variables at time t, and let F_{t-1} be the information set available up to time $t-1$. For notational convenience, the quantile-specific system representation is defined as

$$Y_t(\tau) \equiv Q_\tau(Y_t \mid F_{t-1}) \in \mathbb{R}^m.$$

The QVAR model is defined as follows:

$$Y_t(\tau) = \alpha(\tau) + \sum_{k=1}^{p} \Phi_k(\tau)\, Y_{t-k} + \epsilon_t(\tau), \tag{5.1}$$

where $\alpha(\tau)$ denotes a quantile-specific constant vector of size $m \times 1$; $\Phi_k(\tau)$ represents the $m \times m$ autoregressive coefficient matrix at lag k; and $\epsilon_t(\tau)$ is the error term of size $m \times 1$, satisfying the componentwise quantile restriction $Q_\tau(\epsilon_t(\tau) \mid F_{t-1}) = 0$.

Here, the error term captures quantile-idiosyncratic shocks. To analyze the temporal propagation of shocks within the system, the QVAR model is transformed into a moving-average (VMA) representation, enabling impulse responses and forecast error variance decompositions to be interpreted in a dynamic, quantile-specific manner:

$$Y_t(\tau) \equiv Q_\tau(Y_t \mid F_{t-1}) = \sum_{k=0}^{\infty} \Psi_k(\tau)\, \epsilon_{t-k}(\tau), \tag{5.2}$$

with the contemporaneous coefficient normalized to the identity matrix I_m (i.e., $\Psi_0(\tau) = I_m$); higher-order moving-average coefficients are then generated recursively by premultiplying each autoregressive matrix $\Phi_j(\tau)$ with the obtained coefficient at lag $(k-j)$ and summing over all $j = 1, \ldots, p$ for every $k \geq 1$ [73]. For completeness and reproducibility, Appendix A provides the full mathematical derivations,

from the QVAR(p) specification and check-loss estimation to the VMA recursion, generalized FEVD, and the connectedness measures.

Generalized forecast-error variance decomposition (GFEVD) is used to further investigate spillover effects. GFEVD provides a quantile-specific measure of the extent to which future uncertainty in each variable is attributable to shocks from other variables, thereby quantifying spillover dynamics. Specifically, it decomposes the forecast error variance of each variable over a forecast horizon h into components attributable to shocks from other variables. GFEVD at quantile τ and horizon h is defined as follows:

$$\theta_{ij}^{(\tau)}(h) = \frac{\sigma_{jj}^{-1}(\tau)\sum_{k=0}^{h-1}\left(e_i'\Psi_k(\tau)\,\Sigma(\tau)\,e_j\right)^2}{\sum_{k=0}^{h-1} e_i'\Psi_k(\tau)\,\Sigma(\tau)\,\Psi_k'(\tau)\,e_i}, \qquad i,j=1,\ldots,m, \tag{5.3}$$

where $\Sigma(\tau) = \mathrm{Var}[\epsilon_t(\tau)]$ is the quantile-specific covariance matrix of residuals and $\sigma_{jj}(\tau)$ is its j-th diagonal element (the variance of the j-th shock).

Because $\theta_{ij}^{(\tau)}(h)$ does not guarantee that the elements in each row sum to one, we follow [74] and normalize row-wise:

$$\tilde{\theta}_{ij}^{(\tau)}(h) = \frac{\theta_{ij}^{(\tau)}(h)}{\sum_{r=1}^{m}\theta_{ir}^{(\tau)}(h)}, \qquad \sum_{j=1}^{m}\tilde{\theta}_{ij}^{(\tau)}(h) = 1. \tag{5.4}$$

At a forecast horizon h, the total connectedness index (TCI) for each quantile τ is calculated to assess the dynamics of interdependencies within the system [75]:

$$\mathrm{TCI}^{(\tau)}(h) = \frac{1}{m-1}\sum_{i=1}^{m}\sum_{\substack{j=1\\ j\neq i}}^{m}\tilde{\theta}_{ij}^{(\tau)}(h). \tag{5.5}$$

More explicitly, the total spillover received by variable i from all other variables is defined as

$$F_{i\leftarrow\cdot}^{(\tau)}(h) = \sum_{\substack{j=1\\ j\neq i}}^{m}\tilde{\theta}_{ij}^{(\tau)}(h). \tag{5.6}$$

Following the directional measurement framework proposed by the researchers in [75], we compute the directional spillovers transmitted to others (TO), received from others (FROM), and the net position (NET):

$$\mathrm{TO}_i^{(\tau)}(h) = \sum_{\substack{j=1\\ j\neq i}}^{m}\tilde{\theta}_{ji}^{(\tau)}(h), \tag{5.7}$$

$$\mathrm{FROM}_i^{(\tau)}(h) = \sum_{\substack{j=1\\ j\neq i}}^{m}\tilde{\theta}_{ij}^{(\tau)}(h), \tag{5.8}$$

$$\mathrm{NET}_i^{(\tau)}(h) \quad = \quad \mathrm{TO}_i^{(\tau)}(h) - \mathrm{FROM}_i^{(\tau)}(h). \tag{5.9}$$

Our empirical implementation rigorously adheres to the outlined QVAR spillover methodology. Moreover, to better capture the mechanism linking risk aversion to cross-asset spillovers, we introduce a risk-aversion-centered decomposition that separates the transmission of innovations from the risk-aversion variable to the rest of the system from the absorption of system-wide innovations into risk aversion (see Appendix A for the formal definitions and properties). The lag order ($p = 1$) is selected using the Bayesian information criterion (BIC). Additionally, we employ a rolling-window estimation of 200 trading days to capture the time-varying dynamics.

Importantly, because quantiles are defined relative to the estimation sample within each rolling window, the numerical return cutoff associated with a given quantile level τ can vary over time (e.g., a 75th-quantile cutoff in calm periods may be smaller than that in turmoil periods). Accordingly, τ should be interpreted as a probability-based distributional regime within each window rather than a time-invariant return threshold. The forecast horizon is set to 10 days, and the generalized FEVD methodology is chosen for its robustness and invariance to variable ordering [74, 75]. Moreover, observations containing missing values are excluded through listwise deletion to ensure data integrity and estimation consistency. This comprehensive methodological description ensures the clarity, transparency, and reproducibility of our empirical findings.

Unlike a standard VAR, which characterizes dynamic interactions at the conditional mean, the QVAR models the system at a given quantile level τ of the conditional return distribution. This enables the propagation mechanism to differ across distributional states (e.g., bear vs. bull markets), capturing nonlinearities and asymmetries that are often salient in financial data. In our setting, quantile-specific connectedness measures quantify how shocks transmit *conditional on* a lower-tail, median, or upper-tail regime, rather than describing an average (mean-based) transmission channel. This quantile-based perspective is economically well-motivated because safe-haven behavior and risk transmission are inherently state-dependent; during episodes of stress, tighter funding conditions and liquidity frictions can amplify spillovers, whereas in tranquil periods, cross-market linkages may be weaker. Quantile models provide a parsimonious way to accommodate such state dependence and tail-risk dynamics, which are central to evaluating safe-haven assets under varying levels of risk aversion.

Established theoretical mechanisms in econometrics and finance support the use of quantile models.

First, quantile regression has a clear decision-theoretic interpretation: It characterizes conditional distributional states by minimizing an asymmetric loss function, which is well suited to settings in which downside and upside outcomes are valued differently [76].

Second, theories of funding constraints and liquidity frictions imply that shock propagation can become nonlinear and state-dependent. During stress episodes, tighter funding conditions and liquidity spirals may amplify cross-market transmission, whereas such linkages can be substantially weaker in tranquil periods [77].

These arguments justify focusing on quantile-dependent dynamics when evaluating connectedness and safe-haven properties under varying levels of risk aversion.

Applying a QVAR-based spillover framework enables us to capture the nonlinear and state-dependent effects that emerge under market regimes. This approach enhances our understanding of the complex interdependencies governing risk aversion and asset performance while providing valuable insights for policymakers, portfolio managers, and researchers seeking to identify and manage risks in an increasingly interconnected and unpredictable financial environment.

6. Empirical results

In this section, we presents the pairwise spillover results for the 10%, 50%, and 90% quantiles, which correspond to bear, normal, and bull market conditions, respectively. Because quantiles are defined relative to the estimation sample within each rolling window, the numerical return cutoff associated with a given quantile level can vary over time. Accordingly, these quantile-specific results should be interpreted as state-dependent spillovers across distributional regimes rather than as effects tied to fixed return thresholds. The analyses reveal that the relationships between the variables shift with changing market conditions. For comparisons, Tables 3–5 present the spillover results for each market condition. We also report descriptive statistics and stationarity diagnostics, including the Phillips–Perron test, for all variables to help interpret the empirical results.

6.1. Quantile-based spillover analysis

Table 1 reports summary statistics for the daily returns of 19 variables, including commodities (Au, Ag, Oil), Bitcoin (BTC), major currencies (EUR, GBP, JPY, and CNY), bonds (10Y), the REIT index, dividend stocks (KO, JNJ, T), regional ETFs (KR ETF, JP ETF, US ETF, CN ETF, and EU ETF), and a risk aversion proxy. The statistics include the mean, maximum, minimum, standard deviation, skewness, kurtosis, Jarque–Bera (JB) test for normality, and augmented Dickey–Fuller (ADF) test for stationarity. We also report the Phillips–Perron (PP) unit-root test in Table 1. The PP statistics strongly reject the null hypothesis of a unit root (non-stationarity) for all series at conventional significance levels, which is consistent with the ADF results and supports treating the variables as stationary inputs for the subsequent QVAR-based connectedness analysis.

According to Table 1, Bitcoin (BTC) exhibits the highest mean return (0.003) and volatility (0.04381) among the assets, along with heavy tails (kurtosis = 9.277). Gold (Au) and silver (Ag) exhibit relatively low returns and moderate volatility, with leptokurtic return distributions. Oil exhibits extreme tail behavior, reflecting its susceptibility to large shocks and outliers.

Table 1. Descriptive statistics.

Asset (abbr.)	Mean	Max.	Min.	Std. Dev.	Skewness	Kurtosis	J.-B.	ADF	PP
Gold (Au)	0.00031	0.05948	-0.04979	0.00932	0.021	6.713	1400.31†	-50.83†	-51.09†
Silver (Ag)	0.00035	0.09286	-0.11649	0.01816	-0.245	8.028	2593.15†	-33.88†	-51.75†
Bitcoin (BTC)	0.00300	0.25247	-0.37169	0.04381	0.003	9.292	4023.32†	-27.43†	-50.01†
Crude oil (Oil)	-0.00115	0.37662	-3.05966	0.07320	-31.813	1284.045	167324610.56†	-11.38†	-35.72†
Euro (EUR)	-0.00006	0.03084	-0.02775	0.00517	0.077	5.755	772.80†	-21.66†	-50.70†
Pound (GBP)	-0.00007	0.03791	-0.07604	0.00605	-0.826	16.529	18845.23†	-15.46†	-48.75†
Yen (JPY)	0.00017	0.03322	-0.04552	0.00572	-0.325	7.663	2249.08†	-50.12†	-51.62†
Yuan (CNY)	0.00007	0.02143	-0.02135	0.00311	-0.253	11.936	8120.21†	-58.41†	-50.14†
S&P REIT (REIT)	0.00033	0.08997	-0.17728	0.01319	-1.111	23.367	42671.74†	-15.83†	-52.85†
10yr Treasury (10Y)	0.00069	0.49900	-0.29320	0.03174	1.862	44.616	177458.36†	-8.66†	-35.49†
Dividend Stock KO (KO)	0.00038	0.06480	-0.09672	0.01138	-0.770	13.054	10503.64†	-15.73†	-52.89†
Dividend Stock JNJ (JNJ)	0.00033	0.07998	-0.10038	0.01149	-0.174	12.267	8725.78†	-14.87†	-52.10†
Dividend Stock T (T)	0.00027	0.10022	-0.10406	0.01429	-0.286	11.390	7174.85†	-14.79†	-52.15†
Korea Index ETF (KR ETF)	0.00020	0.12445	-0.15805	0.01515	-0.469	11.874	8081.56†	-16.14†	-52.59†
Japan Index ETF (JR ETF)	0.00029	0.06944	-0.09805	0.01071	-0.433	9.303	4104.94†	-17.12†	-52.27†
USA Index ETF (US ETF)	0.00055	0.09060	-0.10942	0.01116	-0.546	15.728	16576.38†	-15.57†	-52.43†
China Index ETF (CN ETF)	0.00007	0.21241	-0.10291	0.01744	0.697	14.059	12622.51†	-52.87†	-50.48†
Europe Index ETF (EU ETF)	0.00028	0.09057	-0.11778	0.01211	-1.097	17.051	20536.33†	-16.11†	-52.64†
Risk aversion (RA)	0.00226	2.66179	-0.69245	0.08513	19.394	563.997	32289145.53†	-9.51†	-48.63†

Notes: The sample comprises daily observations from July 1, 2014, to July 14, 2024 (N = 2451). Returns are computed as simple arithmetic changes, $r_t = \left(\frac{P_t}{P_{t-1}} - 1\right)$ (reported in decimal form). JB denotes the Jarque–Bera test statistic for normality (H_0: the series is normally distributed). ADF and PP denote the Augmented Dickey–Fuller and Phillips–Perron unit-root test statistics, respectively (H_0: unit root/non-stationarity). † indicates rejection of the corresponding null hypothesis at the 1% significance level.

Major currencies (EUR, GBP, JPY, and CNY) exhibit near-zero mean returns and low volatility, which is with characteristics of developed foreign exchange markets. The 10-year U.S. Treasury yield (10Y) shows elevated volatility, right skewness, and extreme kurtosis, indicating abrupt yield shifts during monetary tightening cycles. The REIT index is characterized by negative skewness and high kurtosis, reflecting downside risks in real estate markets.

Dividend-paying stocks (KO, JNJ, and T) exhibit low returns and volatility, which is with their defensive nature. They also display negative skewness and moderate excess kurtosis. Regional equity ETFs (Korea, Japan, the U.S., China, and Europe) exhibit relatively stable return behaviors. Among them, the China ETF has the highest volatility, whereas the EU ETF shows notable downside risk.

Finally, risk aversion displays substantial positive skewness and extreme kurtosis, capturing its spiky response to market stress. Overall, the ADF, PP, and JB test results show that all series are stationary and deviate significantly from normality.

Table 2. Pearson correlation matrix of returns.

	Au	Ag	BTC	Oil	EUR	GBP	JPY	CNY	REIT	10Y	KO	JNJ	T	KR ETF	JP ETF	US ETF	CN ETF	EU ETF	RA
Au	1.00	0.78	0.08	0.04	0.07	0.03	-0.07	-0.01	0.04	0.10	0.00	0.02	0.03	0.14	0.06	0.02	0.05	0.09	-0.05
Ag	0.78	1.00	0.11	0.07	0.05	0.04	-0.04	-0.03	0.07	0.06	0.02	0.04	0.08	0.24	0.16	0.14	0.15	0.24	-0.14
BTC	0.08	0.11	1.00	0.03	-0.01	-0.04	-0.00	0.03	0.10	0.01	0.10	0.11	0.12	0.17	0.15	0.20	0.12	0.20	-0.22
Oil	0.04	0.07	0.03	1.00	0.01	0.01	-0.02	-0.01	0.03	0.05	0.12	0.07	0.09	0.12	0.08	0.15	0.09	0.14	-0.09
EUR	0.07	0.05	-0.01	0.01	1.00	0.72	0.40	0.23	0.01	-0.08	0.01	0.04	0.03	0.07	0.04	0.02	0.02	0.01	0.01
GBP	0.03	0.04	-0.04	0.01	0.72	1.00	0.23	0.18	0.01	-0.10	0.03	0.04	0.03	0.08	0.07	0.03	0.01	0.02	-0.01
JPY	-0.07	-0.04	-0.00	-0.02	0.40	0.23	1.00	0.10	-0.00	0.25	-0.01	0.06	0.02	0.01	0.01	-0.01	-0.04	-0.01	0.02
CNY	-0.01	-0.03	0.03	-0.01	0.23	0.18	0.10	1.00	0.01	-0.02	-0.00	0.01	0.01	0.05	0.03	0.02	0.00	0.04	-0.03
REIT	0.04	0.07	0.10	0.03	0.01	0.01	-0.00	0.01	1.00	0.07	0.54	0.45	0.46	0.43	0.40	0.56	0.24	0.44	-0.33
10Y	0.10	0.06	0.01	0.05	-0.08	-0.10	0.25	-0.02	0.07	1.00	0.08	0.12	0.10	0.05	0.10	0.14	0.13	0.14	-0.34
KO	0.00	0.02	0.10	0.12	0.01	0.03	-0.01	-0.00	0.54	0.08	1.00	0.60	0.61	0.58	0.49	0.70	0.52	0.73	-0.48
JNJ	0.02	0.04	0.11	0.07	0.04	0.04	0.06	0.01	0.45	0.12	0.60	1.00	0.63	0.51	0.52	0.75	0.42	0.76	-0.47
T	0.03	0.08	0.12	0.09	0.03	0.03	0.02	0.01	0.46	0.10	0.61	0.63	1.00	0.52	0.51	0.75	0.42	0.74	-0.51
KR ETF	0.14	0.24	0.17	0.12	0.07	0.08	0.01	0.05	0.43	0.05	0.58	0.51	0.52	1.00	0.73	0.74	0.62	0.77	-0.33
JP ETF	0.06	0.16	0.15	0.08	0.04	0.07	0.01	0.03	0.40	0.10	0.49	0.52	0.51	0.73	1.00	0.68	0.53	0.72	-0.34
US ETF	0.02	0.14	0.20	0.15	0.02	0.03	-0.01	0.02	0.56	0.14	0.70	0.75	0.75	0.74	0.68	1.00	0.55	0.83	-0.61
CN ETF	0.05	0.15	0.12	0.09	0.02	0.01	-0.04	0.00	0.24	0.13	0.52	0.42	0.42	0.62	0.53	0.55	1.00	0.60	-0.35
EU ETF	0.09	0.24	0.20	0.14	0.01	0.02	-0.01	0.04	0.44	0.14	0.73	0.76	0.74	0.77	0.72	0.83	0.60	1.00	-0.56
RA	-0.05	-0.14	-0.22	-0.09	0.01	-0.01	0.02	-0.03	-0.33	-0.34	-0.48	-0.47	-0.51	-0.33	-0.34	-0.61	-0.35	-0.56	1.00

Notes: Entries report Pearson correlation coefficients computed from daily return series over the full sample; diagonal elements equal one by construction. Variable names and abbreviations follow the data descriptions in the paper.

Table 3. Summary of average spillovers at conditional quantile τ = 10% (horizon (H)=10).

	Au	Ag	BTC	Oil	EUR	GBP	JPY	CNY	REIT	10Y	KO	JNJ	T	KR ETF	JP ETF	US ETF	CN ETF	EU ETF	RA	FROM
Au	14.63	11.93	4.95	1.49	5.25	4.92	4.34	3.96	5.27	2.57	4.68	4.54	4.44	5.95	5.07	4.5	5.08	5.26	1.17	85.37
Ag	11.66	14.48	4.77	1.5	4.62	4.58	4.17	3.64	5.41	3.04	4.64	4.34	4.43	6.38	5.34	5.01	5.29	5.89	0.82	85.53
BTC	5.31	5.23	16.13	1.48	4.53	4.41	4.64	4.32	5.49	3.96	4.77	4.88	4.68	6.1	5.83	6.08	5.58	6.19	0.4	83.88
Oil	3.3	3.55	3.08	35.93	3.23	3.14	3.2	2.39	4.45	3.77	4.05	3.3	3.5	4.64	4.46	4.98	4.06	4.82	0.17	64.09
EUR	6.84	6.18	4.8	1.49	12.18	7.71	3.42	3.71	5.23	3.38	4.94	4.68	4.61	6.49	5.41	5.11	5.72	6.6	1.49	87.81
GBP	6.06	5.85	4.48	1.88	7.57	12.05	3.74	3.45	5.5	3.54	5.13	4.62	4.46	6.48	5.76	5.6	5.75	7.06	1.03	87.96
JPY	6.15	5.36	4.71	1.58	2.79	3.53	16.14	5.21	5.04	5.4	5.17	5.17	4.72	5.81	5.46	5.26	5.06	5.46	1.99	83.87
CNY	6.63	6.25	5.11	1.36	4.83	4.52	5.13	10.92	5.04	4.17	4.79	4.92	4.75	7.17	5.68	5.33	6.24	6.05	1.11	89.08
REIT	4.28	4.56	4.02	1.6	3.27	3.42	3.69	3.16	11.75	3.23	7.46	6.02	6.31	7.22	7.33	8.78	5.76	7.95	0.18	88.24
10Y	2.72	3.4	4.17	2.02	4.24	4.41	5.58	4.04	4.78	17.44	5.49	5.32	5.38	6.06	5.93	6.49	5.61	6.58	0.35	82.57
KO	4.1	4.21	3.67	1.56	3.47	3.59	4.02	3.24	7.95	3.9	12.46	7.11	6.6	6.51	6.81	7.91	5.37	7.35	0.16	87.53
JNJ	4.15	4.09	4.15	1.38	3.97	4.14	4.31	3.31	6.59	3.92	7.3	12.47	6.12	6.44	6.63	7.68	5.7	6.87	0.77	87.52
T	4.08	4.19	4.03	1.53	3.68	3.77	4.1	3.33	7.19	4.06	7.1	6.4	13	6.41	6.67	7.47	5.6	6.99	0.41	87.01
KR ETF	4.4	4.95	4.18	1.54	3.41	3.57	3.9	3.4	6.77	3.92	5.73	5.41	5.21	11.09	8.01	8.04	7.94	8.4	0.14	88.92
JP ETF	3.86	4.25	4.1	1.51	3.32	3.45	3.81	3.12	6.99	3.86	6.09	5.7	5.59	8.17	11.3	8.59	7.18	8.9	0.21	88.7
US ETF	3.39	4.01	4.28	1.74	3.25	3.44	3.65	2.75	7.91	3.97	6.7	6.41	5.94	7.87	8.15	10.59	6.73	8.91	0.32	89.42
CN ETF	4.17	4.57	4.22	1.49	3.79	3.88	3.84	3.17	6.07	3.97	5.33	5.19	5.13	8.86	7.83	7.67	12.35	8.2	0.27	87.65
EU ETF	3.91	4.53	4.27	1.59	3.2	3.44	3.7	2.84	7.23	4.07	6.29	5.65	5.56	8.19	8.49	8.92	7.16	10.81	0.15	89.19
RA	4.23	2.81	2.08	1.81	5.71	5.08	4.47	3.43	2.31	2.51	2.14	2.34	2.38	2.03	2.15	2.7	2.06	2.18	47.59	52.42
TO	89.24	89.92	75.07	28.55	74.13	75	73.71	62.47	105.22	67.24	97.8	92	89.81	116.78	111.01	116.12	101.89	119.66	11.14	
NET	3.87	4.39	-8.81	-35.54	-13.68	-12.96	-10.16	-26.61	16.98	-15.33	10.27	4.48	2.8	27.86	22.31	26.7	14.24	30.47	-41.28	

Notes: "FROM" represents the total spillovers received by the i-th group from all other groups, as defined in Equation (5.8). "TO" refers to the total spillovers transmitted by the i-th group to all other groups, as outlined in Equation (5.7). "NET" indicates the net spillovers, calculated as described in Equation (5.9).

Table 4. Summary of average spillovers at conditional quantile τ = 50%, (H=10).

	Au	Ag	BTC	Oil	EUR	GBP	JPY	CNY	REIT	10Y	KO	JNJ	T	KR ETF	JP ETF	US ETF	CN ETF	EU ETF	RA	FROM
Au	56.44	34.12	0.43	0.13	0.29	0.01	0.29	0.02	0.86	4.32	0.21	0.00	0.05	1.07	0.25	0.18	0.22	0.63	0.49	43.57
Ag	30.73	50.75	0.65	0.38	0.08	0.07	0.12	0.02	2.18	0.72	0.58	0.07	0.43	3.48	1.47	1.53	1.62	3.39	1.73	49.25
BTC	0.61	1.05	80.43	0.10	0.01	0.13	0.00	0.09	1.72	0.01	0.26	0.25	0.44	1.90	1.66	3.20	1.12	3.14	3.86	19.55
Oil	0.07	0.28	0.13	88.28	0.05	0.04	0.09	0.00	1.58	0.81	0.99	0.14	0.35	1.20	1.00	1.63	0.64	1.69	1.02	11.71
EUR	7.18	5.95	0.46	0.06	46.29	9.92	5.92	0.84	1.57	1.09	1.06	0.26	0.44	5.21	1.78	1.25	1.30	9.00	0.41	53.7
GBP	3.17	3.75	0.88	0.23	9.67	45.15	2.25	0.92	3.28	0.20	1.28	0.45	0.95	5.96	4.08	3.52	2.57	10.52	1.16	54.84
JPY	9.53	3.91	0.02	0.11	6.93	2.71	54.50	0.78	0.19	12.11	0.71	0.92	0.55	0.29	0.50	2.63	0.84	0.85	1.91	45.49
CNY	3.01	3.32	0.29	0.08	1.68	1.77	1.02	79.18	0.65	0.08	0.18	0.03	0.09	2.69	0.85	0.76	1.63	2.19	0.49	20.81
REIT	0.40	1.05	0.56	0.62	0.04	0.03	0.05	0.08	27.10	0.32	9.27	4.63	5.53	7.14	8.05	14.02	3.25	10.62	7.24	72.9
10Y	5.10	0.94	0.01	0.80	0.04	0.01	0.48	0.01	0.74	67.03	1.93	1.64	1.82	2.18	2.68	4.73	1.57	4.15	4.15	32.98
KO	0.11	0.38	0.13	0.37	0.08	0.00	0.15	0.03	11.26	1.16	33.13	8.10	6.88	4.60	6.36	11.37	2.00	8.51	5.37	66.86
JNJ	0.04	0.07	0.11	0.08	0.11	0.01	0.12	0.12	6.92	1.35	9.94	40.35	5.80	4.11	5.71	11.51	2.07	6.87	4.70	59.64
T	0.05	0.33	0.22	0.24	0.06	0.03	0.06	0.09	8.30	1.27	8.45	5.81	40.88	4.00	6.19	9.73	2.43	7.33	4.53	59.12
KR ETF	0.49	1.72	0.61	0.39	0.11	0.05	0.09	0.06	7.00	0.78	3.86	2.83	2.69	26.01	11.00	12.34	10.68	13.42	5.87	73.99
JP ETF	0.07	0.68	0.51	0.28	0.07	0.06	0.11	0.03	7.61	1.19	5.11	3.73	4.07	10.61	25.39	13.86	7.18	14.00	5.44	74.61
US ETF	0.02	0.52	0.79	0.44	0.05	0.02	0.09	0.02	10.61	1.42	7.07	5.80	4.91	9.53	11.09	20.54	5.96	13.77	7.38	79.49
CN ETF	0.10	0.95	0.49	0.27	0.10	0.05	0.10	0.02	4.31	1.01	2.47	1.85	2.25	14.42	10.03	10.49	34.98	11.95	4.16	65.02
EU ETF	0.19	1.36	0.84	0.44	0.05	0.04	0.11	0.02	8.53	1.29	5.59	3.65	3.92	11.23	12.06	14.67	7.40	21.84	6.76	78.15
RA	0.13	0.94	1.62	0.41	0.11	0.01	0.19	0.09	8.87	1.26	5.23	2.91	3.41	7.04	6.93	11.90	3.57	10.44	34.95	65.06
TO	61	61.32	8.75	5.43	19.53	14.96	11.24	3.24	86.18	30.39	64.19	43.07	44.58	96.66	91.69	129.32	56.05	132.47	66.67	
NET	17.43	12.07	-10.8	-6.28	-34.17	-39.88	-34.25	-17.57	13.28	-2.59	-2.67	-16.57	-14.54	22.67	17.08	49.83	-8.97	54.32	1.61	

Table 5. Summary of average spillovers at conditional quantile τ = 90%, (H=10).

	Au	Ag	BTC	Oil	EUR	GBP	JPY	CNY	REIT	10Y	KO	JNJ	T	KR ETF	JP ETF	US ETF	CN ETF	EU ETF	RA	FROM
Au	14.79	11.94	5.12	1.49	5.36	4.85	4.13	4.10	5.14	2.64	4.66	4.50	4.57	5.85	5.29	4.68	4.96	5.14	0.81	85.23
Ag	11.54	14.28	4.94	1.44	4.74	4.43	3.93	3.64	5.45	3.05	4.68	4.27	4.45	6.44	5.66	5.25	5.44	6.01	0.35	85.71
BTC	5.42	5.48	15.81	1.23	4.68	4.42	4.64	4.37	5.43	4.29	4.76	4.79	4.87	6.04	5.87	6.09	5.59	6.01	0.21	84.19
Oil	3.45	3.73	2.84	36.56	3.41	2.85	2.97	2.13	4.17	4.46	4.04	3.38	2.98	4.73	4.55	5.15	3.80	4.76	0.05	63.45
EUR	7.17	6.43	5.10	1.21	12.71	7.85	3.09	3.96	4.72	3.87	4.77	4.74	4.73	6.09	5.41	4.96	5.29	6.35	1.55	87.29
GBP	6.00	5.89	4.53	1.45	7.86	12.42	3.77	3.26	5.22	3.88	4.92	4.69	4.85	6.26	5.97	5.62	5.55	6.85	1.02	87.59
JPY	6.75	5.96	5.18	1.34	2.95	3.55	16.36	5.39	4.95	4.86	5.12	5.12	4.77	5.86	5.67	5.00	4.86	5.24	1.06	83.63
CNY	6.05	5.83	4.78	1.14	4.40	4.40	5.19	13.23	5.19	4.15	4.82	4.82	5.09	6.85	6.06	5.56	5.92	5.94	0.58	86.77
REIT	4.14	4.56	4.08	1.36	3.20	3.26	3.40	3.19	12.05	3.35	7.50	6.13	6.26	7.13	7.44	8.94	5.64	7.98	0.38	87.94
10Y	2.95	3.71	4.53	1.96	4.55	4.46	5.09	4.04	4.54	16.32	5.44	5.34	5.40	6.10	6.18	6.45	5.65	6.24	1.06	83.69
KO	3.96	4.20	3.78	1.38	3.53	3.38	3.84	3.30	7.92	4.19	12.73	7.20	6.63	6.44	6.88	8.02	5.20	7.34	0.08	87.27
JNJ	3.97	3.98	3.94	1.27	3.70	3.61	4.10	3.39	6.77	4.41	7.53	13.27	6.27	6.31	6.79	8.06	5.41	6.92	0.29	86.72
T	4.18	4.24	4.15	1.18	3.90	3.81	3.84	3.55	7.00	4.34	7.00	6.36	13.45	6.05	6.71	7.39	5.44	6.77	0.64	86.55
KR ETF	4.35	5.02	4.26	1.46	3.43	3.41	3.74	3.35	6.65	4.23	5.72	5.35	5.07	11.25	8.10	8.20	7.88	8.48	0.05	88.75
JP ETF	3.92	4.44	4.15	1.41	3.40	3.38	3.73	3.25	6.94	4.19	6.07	5.69	5.59	8.07	11.25	8.70	6.98	8.76	0.09	88.76
US ETF	3.32	3.94	4.13	1.55	3.08	3.05	3.38	2.85	8.02	4.28	6.84	6.52	5.95	7.86	8.39	10.86	6.59	8.98	0.43	89.16
CN ETF	4.18	4.71	4.45	1.30	3.86	3.76	3.73	3.21	5.95	4.43	5.22	5.16	5.14	8.82	7.81	7.75	12.44	8.02	0.06	87.56
EU ETF	3.76	4.60	4.16	1.43	3.05	3.10	3.45	2.81	7.30	4.21	6.39	5.70	5.55	8.34	8.63	9.18	7.07	11.08	0.20	88.93
RA	3.83	1.71	1.15	0.08	6.54	4.93	3.50	3.18	0.60	0.98	0.02	0.33	0.21	0.26	0.19	1.07	0.58	0.91	69.93	30.07
TO	88.94	90.37	75.27	23.68	75.64	72.50	69.52	62.97	101.96	69.81	95.50	90.09	88.38	113.50	111.60	116.07	97.85	116.70	8.91	
NET	3.71	4.66	-8.92	-39.77	-11.65	-15.09	-14.11	-23.80	14.02	-13.88	8.23	3.37	1.83	24.75	22.84	26.91	10.29	27.77	-21.16	

Table 2 presents the Pearson correlation matrix of daily returns across the full sample. Correlations are higher within asset classes than across them: Gold and silver exhibit a correlation of 0.78, EUR and GBP of 0.72, and U.S. and European equity ETFs of 0.83. Cross-asset correlations are notably lower, with gold–Bitcoin at 0.08 and gold–oil at 0.04. The RA index is negatively correlated with risk-on assets, with correlations of −0.61 for U.S. equities, −0.56 for European equities, and −0.22 for Bitcoin. These patterns suggest that higher risk aversion coincides with weaker returns on risky assets. However, since correlations do not imply causality or directionality, we use Table 2 as a complementary baseline to the QVAR-based spillover results in Tables 3, 4, and 5, which capture state-dependent transmission patterns.

Table 4 reports the relationship between each asset and global risk aversion under stable market conditions (quantile $\tau = 50\%$). Under normal market conditions, spillovers between assets are relatively balanced; however, certain assets emerge as primary transmitters or receivers of risk. Notably, the Europe Index ETF (EU ETF) and the U.S. Index ETF (US ETF) record the highest TO values, at 132.47 and 129.32, respectively, highlighting their roles as major spillover transmitters in stable markets. This indicates that ETFs significantly influence the transmission of risk aversion across financial networks. Conversely, gold (Au) and silver (Ag), with FROM values of 43.57 and 49.25%, respectively, act as stable recipient assets for investors, reinforcing their status as safe-haven assets that absorb risk during stable periods [41, 50–52].

Additionally, the interaction between EUR and GBP is particularly pronounced under normal market conditions ($\tau = 50\%$), with spillovers of 9.92 from EUR to GBP and 9.67 in return. This finding reflects the strong interconnectedness of major European currencies and their joint role in stabilizing investor sentiment within the Eurozone [5, 61].

Furthermore, the S&P REIT exhibits a TO spillover of 9.27 to Dividend Stock KO, with a FROM spillover of 11.26 in return under normal market conditions. This finding highlights the strengthened link between real estate and dividend stocks under normal market conditions. Tables 3 and 5 present the pairwise spillover results for bear and bull markets, respectively. Compared with normal market conditions, bull (quantile 0.9) and bear (quantile 0.1) markets exhibit increased spillover intensity among specific asset pairs, with TO and FROM values delineating the roles of safe and risky assets. Under bull market conditions ($\tau = 90\%$), high-risk assets such as Bitcoin (BTC) and the S&P REIT serve as major spillover transmitters, with TO values of 75.27 and 101.96, respectively. Notably, Bitcoin generates a spillover of 1.23 to oil, highlighting the intensified interactions among high-risk assets and their collective influence on market dynamics during prosperous periods [44, 53, 62]. Additionally, the S&P REIT shows a TO spillover of 7.50 to Dividend Stock KO, with a FROM spillover of 7.92 in return, emphasizing the reinforced connections between real estate and dividend stocks under bull market conditions. This finding indicates that investors continue to incorporate REITs and dividend-paying stocks to mitigate portfolio risk through diversification [66, 67, 78].

In bear markets, the 10-year Treasury bond (10Y), with a high FROM value of 82.57, serves as a stable safe-haven asset by absorbing substantial spillovers from other assets, reinforcing its crucial role in risk mitigation under distressed conditions [7, 65]. Similarly, gold (Au) records a FROM value of 85.37, further underscoring its status as a reliable safe-haven asset to which investors turn during heightened uncertainty [41, 50]. The pairwise interaction between gold (Au) and the Japanese Yen (JPY) is strengthened in bear markets, with spillovers of 4.34 from gold to Yen and 5.26 from Yen to gold, reflecting increased connectivity among safe-haven assets and their collective role in stabilizing

investor portfolios [5].

Under normal market conditions, Bitcoin (BTC) records a TO value of 8.75, positioning it as a spillover contributor. However, this value increases to 75.07 in bear markets and remains at 75.27 in bull markets, suggesting that Bitcoin acts as a relatively stable spillover source under extreme market conditions. These results indicate that while Bitcoin acts as a risk transmitter during stable periods, its influence remains consistent when markets are booming or in recession, reflecting shifts in investor behavior toward higher-return or safe-haven assets under different conditions [44, 62].

The primary distinction between bull and bear markets is reflected in the TO and FROM values and in the pairwise interactions among safe-haven assets. In bull markets, gold and the S&P REIT emerge as prominent spillover transmitters, with TO values of 88.94 and 101.96, respectively. Notably, a spillover of 5.12 from gold to oil highlights the increased influence of traditional safe-haven assets during economic expansion. In bear markets, the 10-year Treasury bond, with a FROM value of 82.57, and gold, with a FROM value of 85.37, play pivotal roles in absorbing risk spillovers, reaffirming their status as dependable safe-haven assets during periods of heightened uncertainty. The pairwise interaction between gold and Yen is particularly pronounced in bear markets, with spillovers of 4.13 from gold to Yen and 6.15 from Yen to gold, indicating heightened interconnectivity between these assets in stabilizing investor portfolios during market downturns.

Gold and silver consistently exhibit stability across market conditions, reinforcing their reputations as robust safe-haven assets. Gold records FROM values of 85.37 in bear markets, 43.57 in normal markets, and 88.94 in bull markets, maintaining its role as a reliable spillover recipient regardless of market dynamics. Similarly, silver remains stable in bear, normal, and bull markets, with FROM values of 85.53, 49.25, and 85.71, respectively. The risk aversion indicator also reflects consistent investor behavior favoring risk-averse strategies, with FROM values of 52.42 in bear markets, 30.07 in normal markets, and 30.07 in bull markets, underscoring its role in capturing shifts in market sentiment during periods of economic stress [5, 41, 50–52].

In summary, the spillover analysis across quantiles reveals that, even among safe-haven candidates, relationships between assets and global risk aversion are dynamic and depend on market conditions. Assets such as gold, silver, and U.S. Treasuries consistently exhibit strong risk-absorbing characteristics across market states, reaffirming their reputations as reliable safe-haven assets. Conversely, other safe-haven candidates, including the S&P REIT and Bitcoin, demonstrate a higher propensity to transmit risk, particularly during stable and boom conditions. These findings underscore the importance of understanding the nuanced roles of safe-haven assets within diversified portfolios, as their spillover behaviors vary significantly across market environments, influencing the resilience and stability of investment strategies under different levels of risk aversion.

The net spillover shows the dynamic process of shock transmission and reception among diverse asset classes, including equities, bonds, commodities, currencies, and BTC, from 2014 to 2024. This period includes major economic events such as the Brexit referendum (2016–2017), the U.S.–China trade war (2018–2019), the COVID-19 pandemic (2019–2021), and the Federal Reserve's tapering of asset purchases (2022–2023). The analysis employs a rolling-window approach with a window size of 200. Rolling-window estimations are performed across quantiles to capture evolving relationships over time. To provide a benchmark for contemporaneous co-movement among variables, Table 2 reports the pairwise Pearson correlation matrix for the system.

The resulting data are visualized using a net heatmap, which highlights the transmission patterns

of shocks among assets. Sharp intensity shifts in red and blue during specific periods reveal moments when assets transition from shock transmitters to shock receivers, or vice versa, in response to global events such as pandemics, monetary policy adjustments, or changes in international conditions. This analysis is essential for understanding the dynamics of asset interactions as they evolve in response to economic events. The net spillover heatmaps are presented in Figures 2–5, organized by asset class for readability and logical flow, and are interpreted across bear, normal, and bull market regimes.

To strengthen the economic interpretation, the heatmaps in Figures 2–5 are analyzed jointly with the numerical summaries in Tables 2–4, which report net directional positions and identify the leading net transmitters and receivers by quantile. This combined presentation links the time-varying patterns in the heatmaps to the table-based rankings, making regime dependence transparent. In bear markets, the system is characterized by risk-off dynamics, in which hedging demand and flight-to-quality considerations dominate; thus, traditional safe-haven instruments tend to exhibit receiver-like profiles, while spillovers among risky assets intensify. In normal markets, these effects are muted, and net positions are closer to zero, which is consistent with more balanced two-way transmissions. In bull markets, Bitcoin often co-moves with high-risk assets and can appear transmitter-like, which is consistent with the mechanism described in Section 4: Under elevated risk appetite and looser financial constraints, Bitcoin is primarily priced as a speculative, high-beta instrument, and shocks propagate through portfolio rebalancing and liquidity-driven positioning rather than through safe-haven demand.

From an economic perspective, the heatmaps reveal a clear state-dependent *re-ranking* of net spillovers across asset classes. In the lower-tail regime, the patterns are consistent with a risk-off environment, in which funding and margin constraints amplify spillovers among risky assets while increasing hedging demand for traditional safe-haven assets [69, 70]. In contrast, in the upper-tail regime, Bitcoin becomes more closely coupled with high-risk assets, which is consistent with evidence that it frequently behaves as a speculative asset rather than a robust safe haven [35,71,72]. To integrate visual evidence with quantitative interpretation, we report in the main text, alongside each heatmap, the leading net transmitters and receivers and their re-ordering across quantiles, following the tail- and state-dependent connectedness literature [24, 25, 43].

6.2. Time-varying net spillover heatmaps

According to Figures 2–5, which display net heatmaps for major stock indices in the U.S., Europe, and Asia (specifically Figure 5(a)–(e)), stock markets act as shock transmitters. This tendency is particularly pronounced during periods of heightened economic uncertainty, when volatility spreads to other asset classes. For example, Figure 5(c) shows that stock markets acted as strong shock transmitters during events such as the global financial crisis and the COVID-19 pandemic. During these periods, they assume a critical role in transmitting shocks to other assets. This role varies before and after major events; for example, in the early stages of the 2020 pandemic, it functioned as a strong shock transmitter. As the pandemic progressed and relative stability returned, it transitioned to the receiver role, absorbing shocks from other assets. Gold (Figure 3(a)) and Bitcoin exhibit distinct volatility characteristics, revealing contrasting patterns in the net heatmaps. As a traditional safe-haven asset, gold generally serves as a shock receiver, predominantly appearing in blue during financial crises, indicating its role in absorbing shocks from other assets [41, 50].

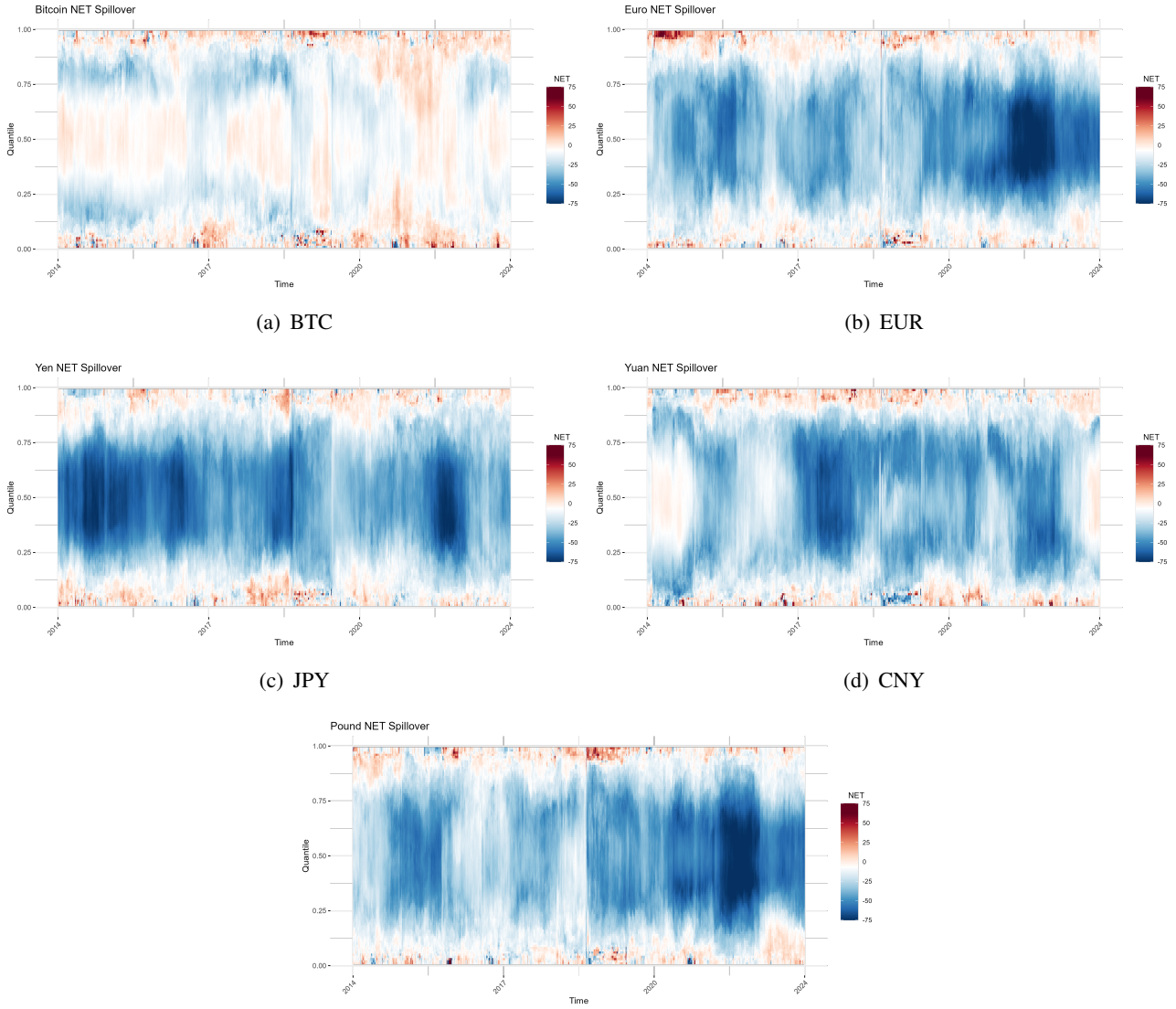

(a) BTC (b) EUR

(c) JPY (d) CNY

(e) GBP

Figure 2. The net spillover index for digital asset and major currencies (Bitcoin, Euro, Yen, Yuan, and Pound). Each panel shows a time–quantile heatmap of the net directional connectedness, defined as $\mathrm{NET}_{i,\tau}(t) = \mathrm{TO}_{i,\tau}(t) - \mathrm{FROM}_{i,\tau}(t)$, computed from the rolling-window QVAR at quantile level $\tau \in (0, 1)$. Warm (red) colors indicate that the asset is a net shock transmitter (NET > 0), whereas cool (blue) colors indicate a net shock receiver (NET < 0). Values close to zero are shown in white, and color intensity increases with |NET| up to 75; values exceeding 75 are displayed using the darkest end of the scale (i.e., the color scale saturates beyond 75). The x-axis is calendar time and the y-axis is the quantile index.

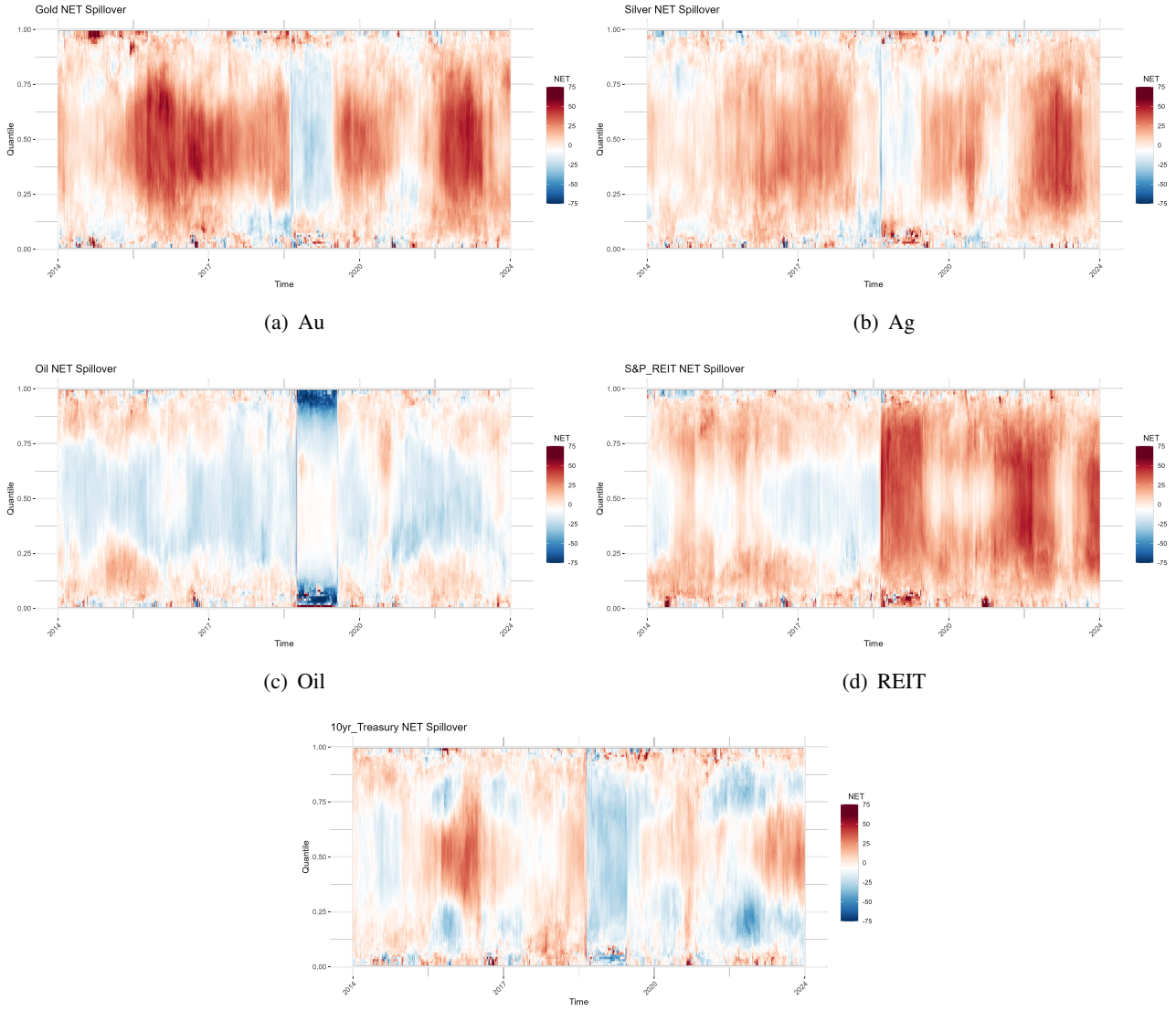

(a) Au (b) Ag

(c) Oil (d) REIT

(e) 10Y

Figure 3. The net spillover index for traditional safe-haven and real asset markets (Gold, Silver, Oil, S&P REIT, and 10yr_Treasury). Each panel shows a time–quantile heatmap of the net directional connectedness, defined as $\mathrm{NET}_{i,\tau}(t) = \mathrm{TO}_{i,\tau}(t) - \mathrm{FROM}_{i,\tau}(t)$, computed from the rolling-window QVAR at quantile level $\tau \in (0, 1)$. Warm (red) colors indicate that the asset is a net shock transmitter (NET > 0), whereas cool (blue) colors indicate a net shock receiver (NET < 0). Values close to zero are shown in white, and color intensity increases with |NET| up to 75; values exceeding 75 are displayed using the darkest end of the scale (i.e., the color scale saturates beyond 75). The x-axis is calendar time and the y-axis is the quantile index.

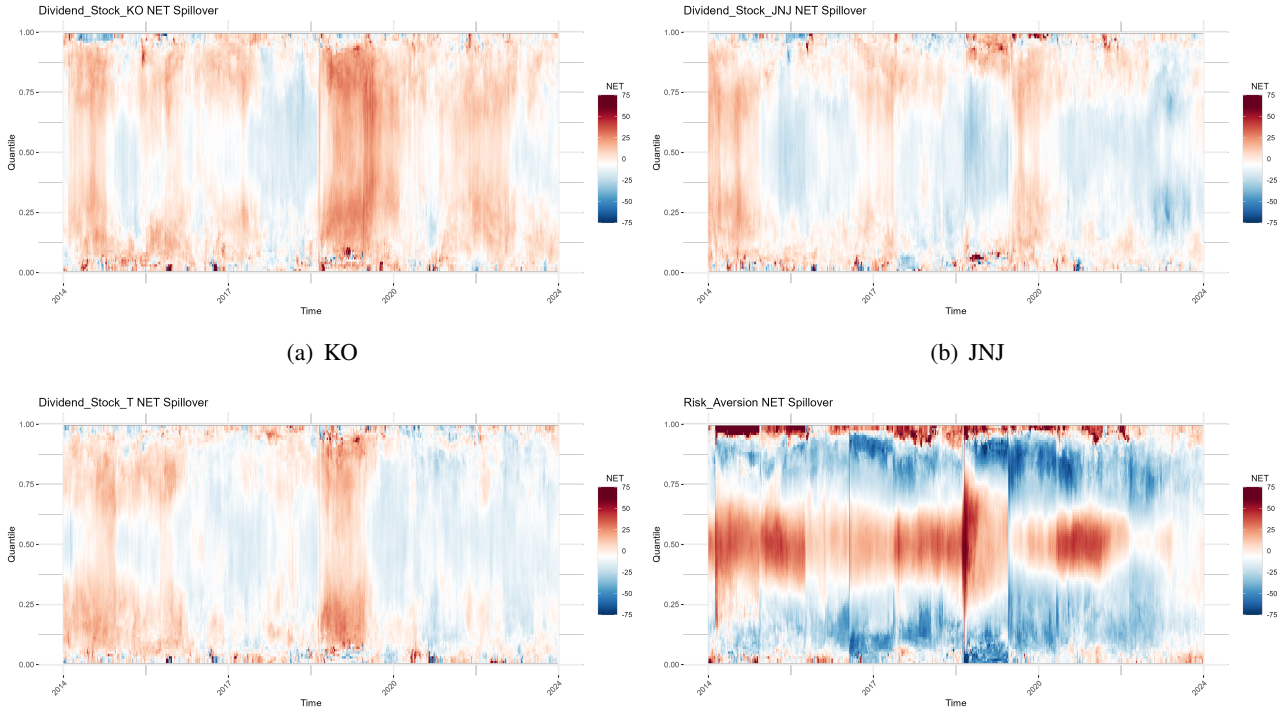

(a) KO (b) JNJ

(c) T (d) RA

Figure 4. The net spillover index for dividend-paying equities and the risk-aversion index (Dividend_Stock_Ko, Dividend_Stock_JNJ, Dividend_Stock_T, and Risk Aversion). Each panel shows a time–quantile heatmap of the net directional connectedness, defined as $\mathrm{NET}_{i,\tau}(t) = \mathrm{TO}_{i,\tau}(t) - \mathrm{FROM}_{i,\tau}(t)$, computed from the rolling-window QVAR at quantile level $\tau \in (0,1)$. Warm (red) colors indicate that the asset is a net shock transmitter (NET > 0), whereas cool (blue) colors indicate a net shock receiver (NET < 0). Values close to zero are shown in white, and color intensity increases with |NET| up to 75; values exceeding 75 are displayed using the darkest end of the scale (i.e., the color scale saturates beyond 75). The x-axis is calendar time and the y-axis is the quantile index.

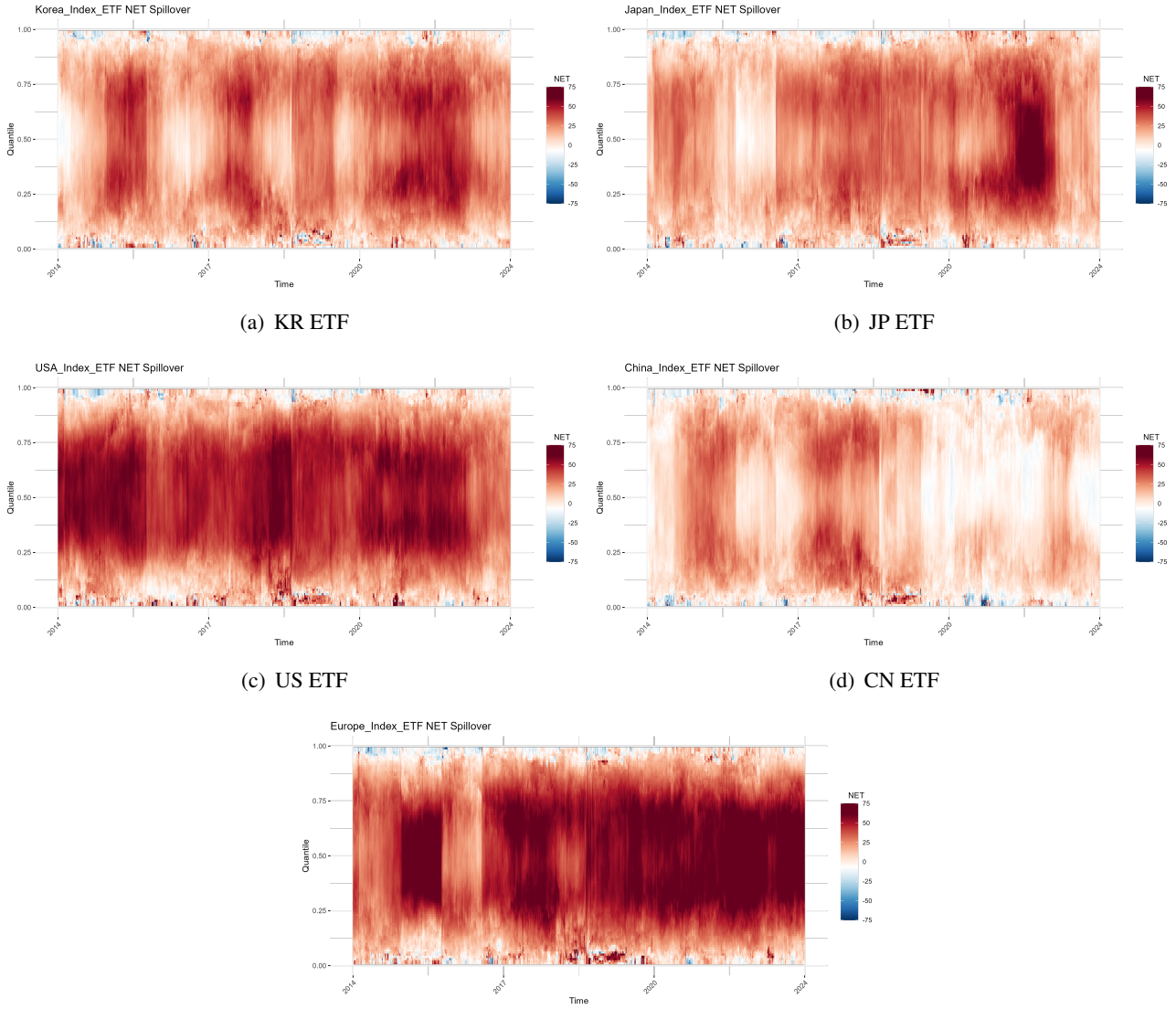

(a) KR ETF (b) JP ETF

(c) US ETF (d) CN ETF

(e) EU ETF

Figure 5. The net spillover index for major regional stock market index ETFs (Korea_Index_ETF, Japan_Index_ETF, USA_Index_ETF, China_Index_ETF, and Europe_Index_ETF). Each panel shows a time–quantile heatmap of the net directional connectedness, defined as $\mathrm{NET}_{i,\tau}(t) = \mathrm{TO}_{i,\tau}(t) - \mathrm{FROM}_{i,\tau}(t)$, computed from the rolling-window QVAR at quantile level $\tau \in (0, 1)$. Warm (red) colors indicate that the asset is a net shock transmitter (NET > 0), whereas cool (blue) colors indicate a net shock receiver (NET < 0). Values close to zero are shown in white, and color intensity increases with |NET| up to 75; values exceeding 75 are displayed using the darkest end of the scale (i.e., the color scale saturates beyond 75). The x-axis is calendar time and the y-axis is the quantile index.

In contrast, Bitcoin exhibits high volatility, alternately functioning as a shock transmitter during certain periods and as a shock receiver in others, thereby playing a dual role in the market. During Bitcoin surges, it acts as a transmitter and imparts shocks to other assets. Conversely, when global

financial instability intensifies, it transitions to a receiver role, responding to shocks from safe-haven assets. These shifts are evident when investors seek to safely diversify assets, suggesting that the time-varying roles of gold and Bitcoin are closely linked to market risk-aversion tendencies. Following Figures 2– 4, currencies and commodities such as the Euro, Yen, and Oil dynamically shift between shock receiver and transmitter roles in response to changes in the international economic environment. Oil prices respond sensitively to major events, such as shifts in international relations or OPEC policies. Occasionally, oil functions as a shock transmitter, imparting shocks to other assets. However, during sharp price declines or supply instabilities, it transitions to a receiver role, absorbing shocks from other assets.

The Euro and Yen predominantly serve as shock receivers during global financial crises and frequently display negative NET values. In response to monetary policy changes, they may temporarily shift to shock-transmitting roles. These transitions demonstrate the sensitivity of each asset to international economic conditions, highlighting the continuously evolving roles of currencies and commodities within a network of interconnected markets. The RAI (Figure 4(d)) and 10-year U.S. Treasury (Figure 3(e)) consistently act as shock receivers across most periods in the net heatmap, although the intensity of their responses varies over time. In recessionary situations, such as a pandemic or global financial crisis, these assets exhibit strongly negative NET values, reinforcing their role in mitigating instability within financial markets by absorbing shocks from other asset classes. As risk aversion decreases and markets stabilize, the intensity of shocks received by these assets diminishes, as reflected in the reduction of the absolute value of their negative NET scores in the heatmap. This suggests that these assets serve as primary shock receivers during high-risk periods. However, as stability returns, their influence on the market diminishes, reflecting weaker interactions with other assets over time [7, 65].

To validate the model's responsiveness to real-world shocks, we explicitly link salient red and blue clusters in Figures 2–5 to major events in our sample. In particular, during the COVID-19 crash in early 2020, the regional equity ETF heatmaps in Figure 5 exhibit intensified red blocks, consistent with heightened shock transmission in stressed markets, while oil in Figure 3 shows a pronounced blue cluster, reflecting the sharp oil-price collapse and receiver-like net positioning. These event-linked patterns are most visible in the bear state and become more muted under normal conditions, whereas several risk-sensitive assets display more transmitter-like behavior in the bull state, which is consistent with the risk-on mechanism discussed in Section 4.

In summary, the spillover analysis across quantiles reveals that the relationship between assets and global risk aversion is dynamic and conditionally dependent. Safe-haven assets such as gold, silver, and U.S. Treasuries consistently absorb risk across market states, whereas high-risk assets such as Bitcoin and the S&P REIT act as significant risk transmitters, mostly during stable and boom conditions. This suggests that gold, silver, and U.S. Treasury securities are consistently regarded as safe-haven assets by market participants, regardless of market conditions. In contrast, Bitcoin is perceived as a prominent asset under bullish market conditions but is not widely recognized as a safe-haven asset during bearish or uncertain periods [35, 38, 72, 79]. These findings underscore the importance of incorporating safe-haven assets into diversified portfolios to mitigate risk across market environments, thereby enhancing the resilience and stability of investment strategies under varying levels of risk aversion.

6.3. Sensitivity and robustness analysis

A robustness test is conducted to validate the QVAR-based spillover analysis. Specifically, we examine the sensitivity of the results to forecast horizon H. Although our main analysis is based on a forecast horizon of $H = 10$, we compare these results with those obtained using alternative values of H to determine whether the differences are statistically significant.

First, to assess the robustness of the spillover analysis over the period, we compute the TCI (5.5) across values of the forecast horizon H for each quantile. As shown in Figure 6, the variation in TCI across H values appears minimal, suggesting that the results are not sensitive to the choice of forecast horizon H.

Figure 7 provides additional evidence of horizon-invariant spillovers by plotting the ratio of TCI values at shorter and longer forecast horizons $H = 5$ and $H = 15$ relative to the benchmark horizon $H = 10$. Except for the most extreme lower-tail quantiles, these ratios are close to unity across the 1 to 99 percentile range, indicating that the connectedness estimates are largely insensitive to the choice of horizon. The minor deviations observed in the lowest quantiles indicate that the robustness documented in Figure 6 extends to almost the full distribution of market states.

Second, Figure 8 illustrates the time-varying behavior of the TCI across the 0.1, 0.5, and 0.9 quantiles. The most notable distinction among the subfigures is that TCI levels observed under extreme market conditions, represented by the 0.1 and 0.9 quantiles, are generally higher than those under median market conditions (0.5 quantile). This finding suggests that shock transmissions across assets intensify during extreme market stress.

Despite differences in magnitude, several common patterns emerge across all three quantiles. First, we find evidence of time-varying systemic interconnectedness across quantile states. Notably, a sharp spike in the TCI in early 2020 coincided with the outbreak of the COVID-19 pandemic. This surge reflects an abrupt intensification of shock transmission among safe-haven assets, driven by heightened uncertainty and synchronized market responses during a systemic crisis. Second, periods of relatively low interconnectedness, such as mid-2017 and late 2023, indicate episodes in which asset markets moved more independently, implying a reduction in systemic spillover risk. These intervals are likely associated with a stable macroeconomic environment or the absence of major global shocks. Third, the persistence of elevated TCI values following systemic events, particularly from 2020 to 2021, highlights the prolonged nature of market interconnectedness in response to global uncertainty. This finding underscores the critical role of exogenous shocks in generating a temporal clustering of spillover intensity.

Overall, Figures 6 and 8 empirically support our choice of setting the forecast horizon at $H = 10$ in the QVAR-based spillover analysis.

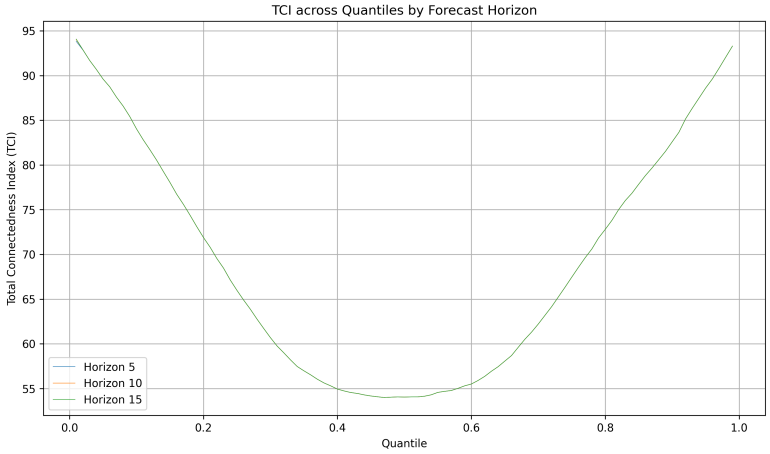

Figure 6. Total connectedness index (TCI) across quantile levels $\tau = 0.01$ to 0.99 for forecast horizons h = 5, 10, and 15. The results demonstrate a consistent U-shaped pattern across all horizons, indicating the robustness of the quantile-dependent connectedness dynamics. To improve visual clarity, a slight horizontal offset is applied between the lines.

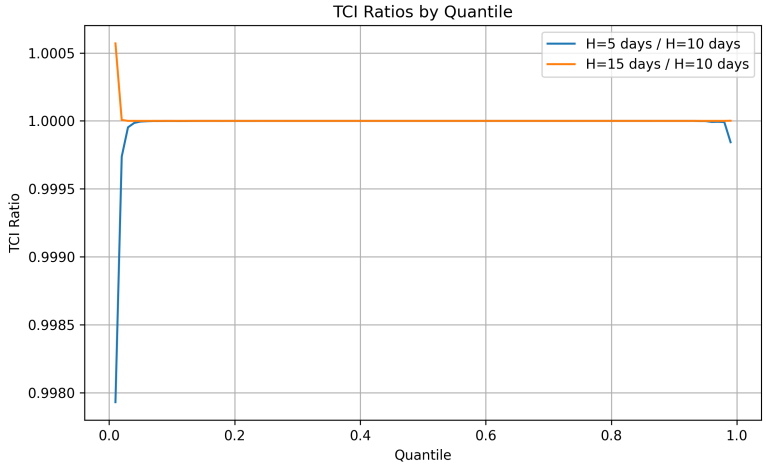

Figure 7. TCI ratios for forecast horizons $H = 5$ days and $H = 15$ days relative to the baseline $H = 10$ days across quantiles. Values close to 1 indicate that connectedness is largely horizon invariant.

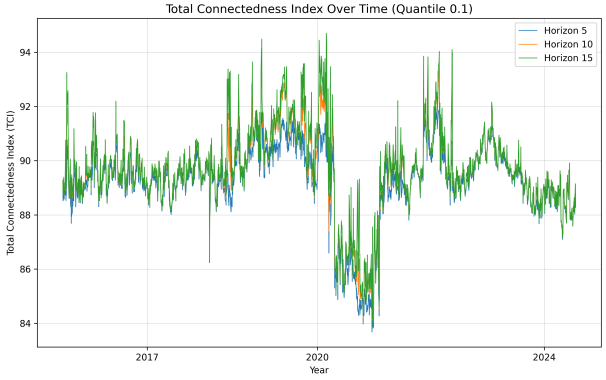

(a) Quantile $\tau = 0.1$

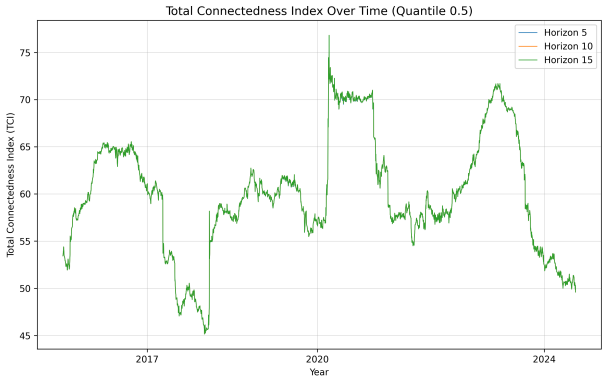

(b) Quantile $\tau = 0.5$

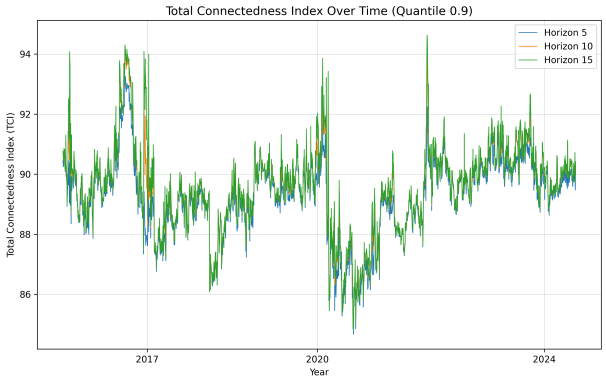

(c) Quantile $\tau = 0.9$

Figure 8. Rolling-window estimation of the total connectedness index (TCI) across quantile levels ($\tau = 0.1, 0.5$, and 0.9), with a window size of 200 trading days. Each subfigure shows the TCI dynamics for three forecast horizons ($H = 5$, $H = 10$, and $H = 15$), capturing variations in connectedness across short-, medium-, and long-term perspectives under different market conditions, respectively.

In addition to the RAI proposed by the researchers in [22], several alternative proxies exist for investor risk aversion. For instance, the VIX has been widely used in the literature as a measure of

equity market participants' risk aversion [32,80,81]. To examine the potential differences arising from alternative risk-aversion measures, we replace the baseline RAI with the VIX and re-estimate the net spillovers using the same forecast horizons (H = 5, 10, and 15) and quantile levels (τ = 0.10, 0.50, and 0.90). The net spillover results are presented in Figures 9–11.

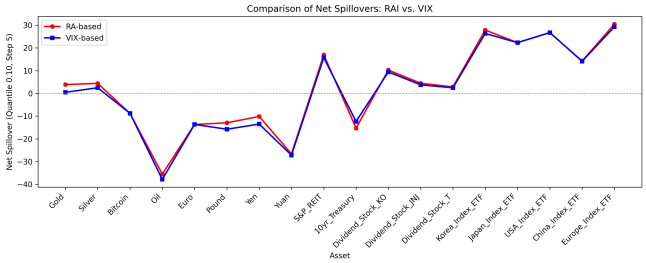

(a) H = 5

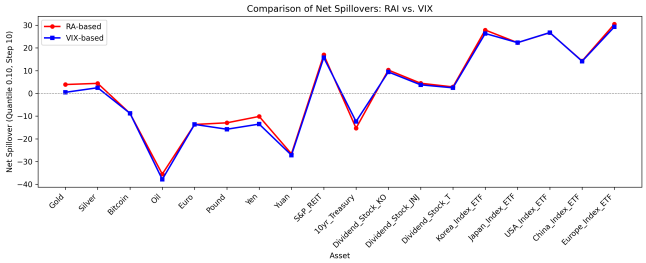

(b) H = 10

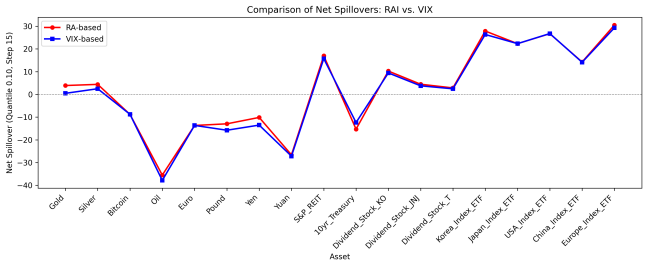

(c) H = 15

Figure 9. Net spillover comparison between the RAI and VIX. Each panel displays net spillover estimates based on the baseline Risk Aversion Index (RAI, red) and the VIX (blue) for a given forecast horizon H at the lower quantile level τ = 0.1. Positive (negative) values indicate that the asset serves as a net transmitter (receiver) of shocks. Assets are ordered from Gold to Europe_Index_ETF, following the sequence in Table A.1.

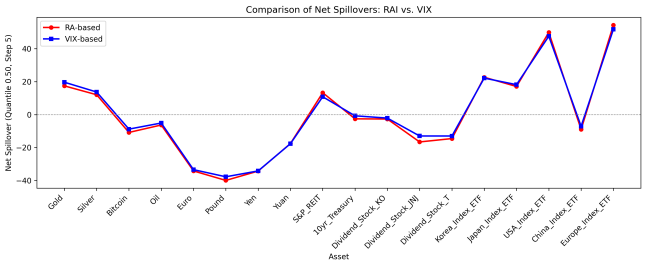

(a) $H = 5$

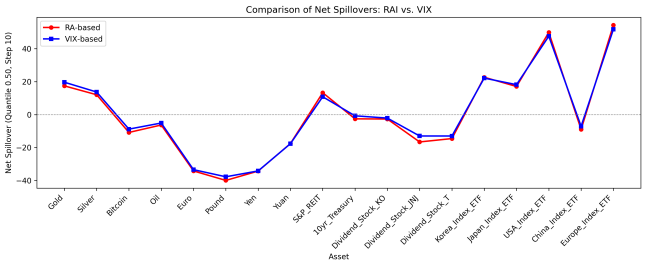

(b) $H = 10$

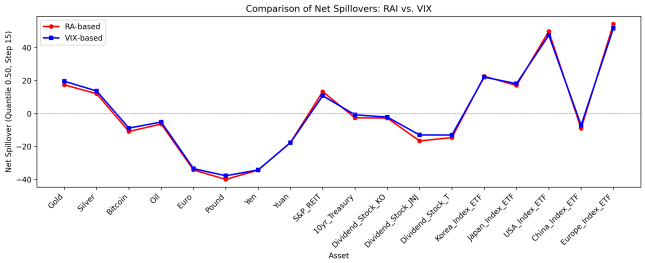

(c) $H = 15$

Figure 10. Net spillover comparison between RAI and VIX. Each panel displays net spillover estimates based on the baseline Risk Aversion Index (RAI, red) and the VIX (blue) for a given forecast horizon H at the lower quantile level $\tau = 0.5$.

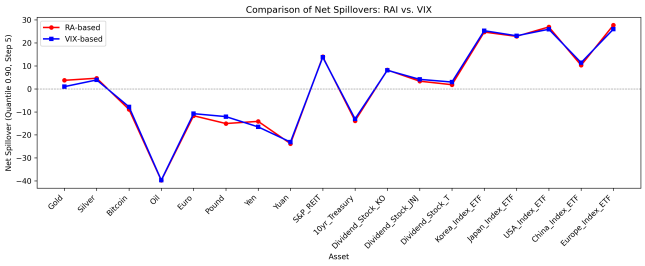

(a) $H = 5$

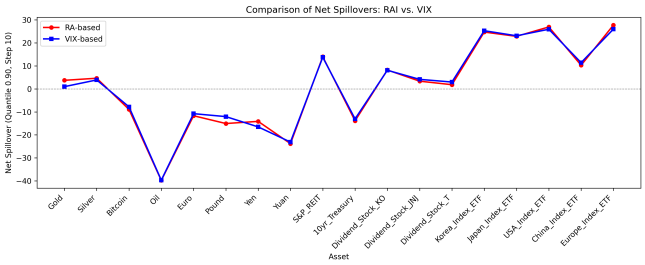

(b) $H = 10$

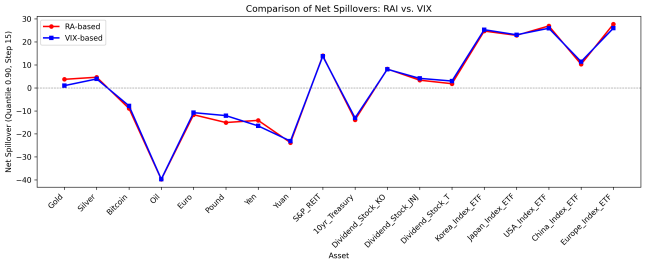

(c) $H = 15$

Figure 11. Net spillover comparison between RAI and VIX. Each panel displays net spillover estimates based on the baseline Risk Aversion Index (RAI, red) and the VIX (blue) for a given forecast horizon H at the lower quantile level $\tau = 0.9$.

The results based on the VIX show strong alignment with those from the baseline measure, revealing consistent spillover patterns across assets and quantiles despite minor differences in absolute values. Moreover, both proxies indicate heightened spillovers under extreme market conditions, reaffirming the intensification of systemic connectedness during periods of stress or exuberance. These findings support the robustness of our results and demonstrate the effectiveness of both measures in capturing market fear and uncertainty.

7. Discussion

7.1. Economic implications

Our findings provide important economic insights into the propagation of risk-aversion across financial markets under different regimes. Consistent with the literature on state-dependent safe-haven behavior [7, 10, 41], traditional safe-haven assets, particularly gold and U.S. Treasuries, act as net

absorbers of risk-aversion shocks in the lower tail of the return distribution. This behavior indicates that, during periods of severe market stress, capital reallocation toward these assets mitigates systemic risk transmission and enhances market stability.

The quantile-specific patterns can be explained by regime-dependent portfolio rebalancing and liquidity conditions. In the lower tail, heightened risk aversion typically triggers flight-to-quality and precautionary liquidity demand, reallocating capital away from risky assets toward high-quality liquid instruments. Consequently, U.S. Treasuries and gold tend to absorb shocks (net receivers), while riskier assets transmit shocks more strongly. In the upper tail, risk-on sentiment, leverage expansion, and stronger co-movement among high-beta assets can amplify cross-market transmission, explaining why Bitcoin and other pro-cyclical assets may appear as net transmitters in median-to-upper quantiles. This stress-versus-risk-on switching mechanism aligns with evidence from quantile connectedness studies, which show stronger and more asymmetric spillovers in tail regimes and role changes between transmitters and receivers across quantiles in cryptocurrency and commodity-related systems [19, 25, 26]. Similar quantile-dependent transmission has been documented in monetary policy-related markets [23] and in regime- and frequency-dependent connectedness of sustainable and clean-energy assets [24]. Our contribution includes documenting and interpreting these regime-dependent propagation channels in a system explicitly conditioned on a global RAI that spans multiple safe-haven candidates across asset classes.

In contrast, Bitcoin and REITs exhibit pronounced regime-dependent dynamics. Bitcoin functions as a dominant net transmitter of risk-aversion shocks under normal and bullish market conditions, reinforcing its characterization as a speculative or high-beta asset rather than a consistent safe haven [34, 37, 44]. Importantly, Bitcoin's spillover influence weakens sharply in the lower tail, suggesting that its diversification benefits deteriorate when downside protection is most valuable. This asymmetric behavior highlights the limitations of viewing Bitcoin as a crisis hedge and underscores its sensitivity to market regimes.

7.2. Policy implications

The distinction between lower- and upper-tail spillovers has direct implications for financial stability and regulatory oversight. Lower-tail spillovers capture downside systemic risk, in which adverse shocks can trigger cascading losses and threaten market functioning. Our evidence that gold and government bonds absorb risk in this regime supports the role of deep and liquid sovereign bond and commodity markets as stabilizing anchors during crises. From a policy perspective, maintaining liquidity and preventing market dysfunction in these assets are critical for mitigating systemic risk.

In contrast, upper-tail spillovers reflect periods of heightened risk-taking and market exuberance. The strong spillover transmission from Bitcoin and equity-related assets during bullish regimes suggests that speculative capital flows intensify market interconnectedness and may amplify boom–bust cycles. Therefore, monitoring upper-tail spillovers can provide early warning signals of excessive leverage, speculative behavior, and emerging asset price bubbles. Incorporating tail-sensitive spillover measures into macroprudential frameworks can enhance regulators' ability to detect and manage systemic vulnerabilities.

7.3. Portfolio implications

From a portfolio management perspective, our results underscore the importance of accounting for state-dependent risk transmission across assets. Under stable and bullish market conditions, Bitcoin acts as a major transmitter of risk-aversion spillovers, implying that its price movements can substantially influence overall portfolio risk while offering return-enhancing opportunities during market upswings [82]. Accordingly, institutional investors may view Bitcoin as a tactical asset in expansionary regimes, provided that its spillover effects are carefully monitored.

In contrast, during downturns, Bitcoin becomes a source of risk transmission, while traditional safe-haven assets, such as gold and U.S. Treasury bonds, serve as effective shock absorbers. This finding suggests that dynamic portfolio rebalancing (reducing exposure to Bitcoin and increasing allocations to safe-haven assets during periods of elevated risk aversion) can enhance downside protection and risk-adjusted performance [82, 83]. Overall, these results highlight the importance of regime-aware and tail-sensitive allocation strategies for institutional investors operating in increasingly interconnected financial markets.

8. Concluding remarks

In this study, we comprehensively analyze the dynamic interplay between global risk aversion and the returns of safe-haven assets using a quantile spillover framework. By employing a QVAR-based spillover approach, we capture the nuanced relationships across quantiles of the conditional return distribution. Our analysis covers a broad range of assets, including gold, silver, Bitcoin, crude oil, major currencies, REITs, U.S. Treasury bonds, dividend-paying stocks, and equity market indices, from July 2014 to July 2024, yielding significant insights into how these assets interact under varying market conditions.

Under stable market conditions (50th quantile), Bitcoin emerges as a dominant spillover transmitter, exerting a significant influence on the transmission of risk aversion across financial networks. This underscores Bitcoin's pivotal role in shaping broader market risk dynamics. In contrast, traditional safe-haven assets such as gold and silver primarily act as risk absorbers, maintaining their roles as refuges of stability. During bull market periods (90th quantile), Bitcoin, alongside higher-risk assets, such as REITs, amplifies its influence as a risk transmitter, further impacting other asset classes and demonstrating its heightened interconnectivity during market upswings. Even in bear market periods (10th quantile), when U.S. Treasury bonds and gold emerge as reliable shock absorbers, Bitcoin's role as a risk transmitter is noteworthy. These findings emphasize the state-dependent nature of asset interdependencies, highlighting Bitcoin's evolving role in financial markets and its critical implications for portfolio diversification and risk management.

Despite providing robust insights, this study has several limitations. First, the analysis period (2014–2024) does not capture the most recent financial market developments, including emerging asset classes. In future research, researchers could extend the analysis by incorporating novel digital assets, such as non-fungible tokens (NFTs), decentralized finance (DeFi) products, and central bank digital currencies (CBDCs), as well as a broader set of safe-haven candidates, including sector-specific ETFs (e.g., utilities, food, and healthcare), additional commodities, and ESG-related assets.

Second, while we employ the RAI proposed by the researchers in [22], alternative proxies, such as the VIX, credit default swap (CDS) spreads [84–86], and investor sentiment indices [87–89], have

been widely used to measure investor risk aversion and may provide complementary information.

Finally, although the rolling-window QVAR-based spillover framework effectively captures time-varying spillover patterns, researchers could consider models that explicitly incorporate parameter evolution, such as time-varying parameter VAR (TVP-VAR) frameworks, to provide a more rigorous representation of dynamic spillover effects.

Overall, this study makes meaningful contributions to the literature on risk management and asset allocation. These findings have valuable implications for academic researchers and industry practitioners seeking to optimize investment strategies in an increasingly complex and interconnected financial landscape.

Appendix

A. Definitions of variables

Table A.1. Asset descriptions, abbreviations, and data sources.

Variable Name	Description	Abbreviation
Gold	Gold prices from COMEX.	Au
Silver	Silver prices from COMEX.	Ag
Bitcoin	Bitcoin prices from cryptocurrency markets.	BTC
Oil	Crude oil prices from NYMEX.	Oil
Euro	Euro to US Dollar exchange rate from forex markets.	EUR
Pound	British Pound to US Dollar exchange rate from forex markets.	GBP
Yen	US Dollar to Japanese Yen exchange rate from forex markets.	JPY
Yuan	US Dollar to Chinese Yuan exchange rate from forex markets.	CNY
S&P_REIT	Vanguard Real Estate ETF data representing US REIT.	REIT
10yr_Treasury	US 10-Year Treasury yield data from US Treasury markets.	10Y
Dividend_Stock_KO	Coca-Cola stock prices from equity markets.	KO
Dividend_Stock_JNJ	Johnson & Johnson stock prices from equity markets.	JNJ
Dividend_Stock_T	AT&T stock prices from equity markets.	T
Korea_Index_ETF	iShares MSCI South Korea ETF.	KR ETF
Japan_Index_ETF	iShares MSCI Japan ETF.	JP ETF
USA_Index_ETF	SPDR S&P 500 ETF Trust.	US ETF
China_Index_ETF	iShares China Large-Cap ETF.	CN ETF
Europe_Index_ETF	Vanguard FTSE Europe ETF.	EU ETF
Risk Aversion	Nancy Xu's Risk Aversion index.	RA

Notes: This table lists the full variable names, their descriptions, and abbreviations. The abbreviations are used consistently across all figures and tables, including the spillover analyses at different quantiles.

B. Mathematical details of the QVAR-based spillover framework

B.1. QVAR specification and estimation

Let $\{Y_t\}_{t=1}^n$ be an $m\times 1$ vector collecting the USD-denominated return series in the system (including the risk-aversion proxy as one of the variables), and let $\mathcal{F}_{t-1}$ denote the information set up to time $t-1$. For a quantile level $\tau \in (0,1)$, the QVAR(p) is specified as

$$Y_t = \alpha(\tau) + \sum_{k=1}^{p} \Phi_k(\tau)\, Y_{t-k} + \varepsilon_t(\tau), \qquad t = p+1, \ldots, n, \tag{B.1}$$

with the componentwise quantile restriction

$$Q_\tau\big(\varepsilon_t(\tau) \mid \mathcal{F}_{t-1}\big) = 0. \tag{B.2}$$

Equivalently,

$$Q_\tau\big(Y_t \mid \mathcal{F}_{t-1}\big) = \alpha(\tau) + \sum_{k=1}^{p} \Phi_k(\tau)\, Y_{t-k}. \tag{B.3}$$

Estimation proceeds equation-by-equation via quantile regression. For each $i = 1, \ldots, m$,

$$\widehat{\beta}_i(\tau) = \arg\min_{\beta} \sum_{t=p+1}^{n} \rho_\tau(y_{i,t} - X_t^\top \beta)\,, \qquad \rho_\tau(u) = u(\tau - \mathbf{1}\{u<0\}), \tag{B.4}$$

where $X_t = [1, Y_{t-1}^\top, \ldots, Y_{t-p}^\top]^\top$. Collecting $\{\widehat{\beta}_i(\tau)\}_{i=1}^m$ yields $\widehat{\alpha}(\tau)$ and $\{\widehat{\Phi}_k(\tau)\}_{k=1}^p$. Define fitted residuals

$$\widehat{\varepsilon}_t(\tau) = Y_t - \widehat{\alpha}(\tau) - \sum_{k=1}^{p} \widehat{\Phi}_k(\tau)\, Y_{t-k}, \qquad t = p+1, \ldots, n, \tag{B.5}$$

and the (plug-in) innovation covariance estimator

$$\widehat{\Sigma}(\tau) = \frac{1}{n-p} \sum_{t=p+1}^{n} \widehat{\varepsilon}_t(\tau)\widehat{\varepsilon}_t(\tau)^\top. \tag{B.6}$$

B.2. Quantile-indexed impulse responses

For each fixed τ, the estimated coefficient matrices $\{\widehat{\Phi}_k(\tau)\}$ define a τ-indexed linear system. Under standard stability conditions for this system, it admits a moving-average representation

$$Y_t = \sum_{k=0}^{\infty} \Psi_k(\tau)\, \varepsilon_{t-k}(\tau), \qquad \Psi_0(\tau) = I_m, \tag{B.7}$$

where $\{\Psi_k(\tau)\}$ are obtained recursively from $\{\Phi_k(\tau)\}$ (in practice, we use the plug-in estimates). This provides the quantile-indexed impulse responses used for the variance decomposition below.

B.3. Generalized FEVD and connectedness measures

Let e_i denote the $m \times 1$ selection vector with 1 in position i and zero otherwise. Let $\Sigma(\tau) = \mathrm{Var}(\varepsilon_t(\tau))$ with diagonal entries $\sigma_{jj}(\tau)$. Assume $\Sigma(\tau)$ is positive semidefinite with $\sigma_{jj}(\tau) > 0$, so that the denominators below are strictly positive. For a forecast horizon $h \in \mathbb{N}$, the generalized FEVD at quantile τ is:

$$\theta_{ij}^{(\tau)}(h) = \frac{\sigma_{jj}^{-1}(\tau) \sum_{k=0}^{h-1} \left(e_i^\top \Psi_k(\tau) \Sigma(\tau) e_j \right)^2}{\sum_{k=0}^{h-1} e_i^\top \Psi_k(\tau) \Sigma(\tau) \Psi_k(\tau)^\top e_i}, \qquad i, j = 1, \ldots, m, \tag{B.8}$$

which is normalized row-wise as

$$\widetilde{\theta}_{ij}^{(\tau)}(h) = \frac{\theta_{ij}^{(\tau)}(h)}{\sum_{\ell=1}^{m} \theta_{i\ell}^{(\tau)}(h)}, \qquad \sum_{j=1}^{m} \widetilde{\theta}_{ij}^{(\tau)}(h) = 1. \tag{B.9}$$

In the implementation, we plug in $\widehat{\Psi}_k(\tau)$ and $\widehat{\Sigma}(\tau)$.

We compute standard connectedness measures. The total connectedness index (TCI) is defined as the average off-diagonal share:

$$\mathrm{TCI}^{(\tau)}(h) = \frac{1}{m} \sum_{i=1}^{m} \sum_{\substack{j=1 \\ j \neq i}}^{m} \widetilde{\theta}_{ij}^{(\tau)}(h). \tag{B.10}$$

Directional spillovers transmitted to others (TO), received from others (FROM), and the net position (NET) are

$$\mathrm{TO}_i^{(\tau)}(h) = \sum_{\substack{j=1 \\ j \neq i}}^{m} \widetilde{\theta}_{ji}^{(\tau)}(h), \tag{B.11}$$

$$\mathrm{FROM}_i^{(\tau)}(h) = \sum_{\substack{j=1 \\ j \neq i}}^{m} \widetilde{\theta}_{ij}^{(\tau)}(h), \tag{B.12}$$

$$\mathrm{NET}_i^{(\tau)}(h) = \mathrm{TO}_i^{(\tau)}(h) - \mathrm{FROM}_i^{(\tau)}(h). \tag{B.13}$$

B.4. Risk-aversion-centered decomposition

Let $r \in \{1, \ldots, m\}$ denote the index of the risk-aversion variable and $S = \{1, \ldots, m\} \setminus \{r\}$. We define two directional channels involving risk aversion:

$$\mathrm{TCI}_{\mathrm{RA} \to \mathrm{SYS}}^{(\tau)}(h) = \frac{1}{m-1} \sum_{i \in S} \widetilde{\theta}_{ir}^{(\tau)}(h), \tag{B.14}$$

$$\mathrm{TCI}_{\mathrm{SYS} \to \mathrm{RA}}^{(\tau)}(h) = \sum_{j \in S} \widetilde{\theta}_{rj}^{(\tau)}(h) = \mathrm{FROM}_r^{(\tau)}(h), \tag{B.15}$$

and the net risk-aversion position

$$\mathrm{NET}_{\mathrm{RA}}^{(\tau)}(h) = \mathrm{NET}_r^{(\tau)}(h) = \mathrm{TO}_r^{(\tau)}(h) - \mathrm{FROM}_r^{(\tau)}(h). \tag{B.16}$$

B.5. Basic properties (by construction)

From (B.8) and (B.9), $\theta_{ij}^{(\tau)}(h) \geq 0$ and $0 \leq \widetilde{\theta}_{ij}^{(\tau)}(h) \leq 1$, with $\sum_{j=1}^{m} \widetilde{\theta}_{ij}^{(\tau)}(h) = 1$ for each i. Consequently, $0 \leq \mathrm{TCI}^{(\tau)}(h) \leq 1$. Moreover, the net connectedness is zero-sum:

$$\sum_{i=1}^{m} \mathrm{NET}_{i}^{(\tau)}(h) = 0, \tag{B.17}$$

since $\sum_i \mathrm{TO}_i^{(\tau)}(h) = \sum_i \mathrm{FROM}_i^{(\tau)}(h)$ by definition [73–75].

Author contributions

H. Choi and S.-Y. Choi: Conceptualization, supervision; S. H. Choi and S.-Y. Choi: Methodology; S. H. Choi, H. Choi, and S.-Y. Choi: Formal analysis, investigation, writing – original draft, writing – review & Eediting; S. H. Choi: Data curation, visualization. All authors have read and approved the final version of the manuscript for publication.

Use of Generative-AI tools declaration

The authors declare they have not used Artificial Intelligence (AI) tools in the creation of this article.

Acknowledgments

The work of H. Choi and S. H. Choi were supported by the National Research Foundation of Korea(NRF) grant funded by the Korean government(MSIT) (No. 2022R1A5A1033624 & RS-2024-00342939). The work of S.-Y. Choi was supported by the National Research Foundation of Korea (NRF) grant funded by the Korean Government (MSIT) (No. RS-2024-00454493).

Conflict of interest

Prof. Sun-Yong Choi is the Guest Editor of special issue "Recent Advances in Mathematical Modeling of Financial Economics" for AIMS Mathematics. Prof. Sun-Yong Choi was not involved in the editorial review and the decision to publish this article. All authors declare no conflicts of interest in this paper.

References

1. J. A. Carlson, Risk aversion, foreign exchange speculation and gambler's ruin, *Economica*, **65** (1998), 441–453. https://doi.org/10.1111/1468-0335.00138
2. R. S. Pindyck, *Risk aversion and determinants of stock market behavior*, Working Paper, 1986.
3. K. Kassimatis, Risk aversion with local risk seeking and stock returns: Evidence from the uk market, *J. Bus. Finan. Account.*, **38** (2011), 713–739. https://doi.org/10.1111/j.1468-5957.2011.02243.x

4. G. Gorton, G. Ordonez, The supply and demand for safe assets, *J. Monetary Econ.*, **125** (2022), 132–147. https://doi.org/10.1016/j.jmoneco.2021.07.010

5. E. Feder-Sempach, P. Szczepocki, J. Bogoebska, Global uncertainty and potential shelters: Gold, bitcoin, and currencies as weak and strong safe havens for main world stock markets, *Financ. Innov.*, **10** (2024), 67. https://doi.org/10.1186/s40854-023-00589-w

6. F. Le Grand, X. Ragot, Sovereign default and liquidity: The case for a world safe asset, *J. Int. Econ.*, **131** (2021), 103462. https://doi.org/10.1016/j.jinteco.2021.103462

7. Z. He, A. Krishnamurthy, K. Milbradt, What makes us government bonds safe assets?, *Am. Econ. Rev.*, **106** (2016), 519–523. https://doi.org/10.1257/aer.p20161109

8. T. Bettendorf, R. Heinlein, Connectedness between G10 currencies: Searching for the causal structure, *Int. J. Finan. Econ.*, **28** (2023), 3938–3959. https://doi.org/10.1002/ijfe.2629

9. Z. Umar, A. Bossman, S. Y. Choi, T. Teplova, The relationship between global risk aversion and returns from safe-haven assets, *Financ. Res. Lett.*, **51** (2023), 103444. https://doi.org/10.1016/j.frl.2022.103444

10. D. G. Baur, T. Dimpfl, K. Kuck, *Safe haven assets-the bigger picture*, Available at SSRN 3800872, 2021. https://doi.org/10.2139/ssrn.3800872

11. C. Gurdgiev, A. Petrovskiy, Hedging and safe haven assets dynamics in developed and developing markets: Are different markets that much different?, *Int. Rev. Financ. Anal.*, **92** (2024), 103059. https://doi.org/10.1016/j.irfa.2023.103059

12. R. Khalfaoui, S. B. Jabeur, B. Dogan, The spillover effects and connectedness among green commodities, Bitcoins, and us stock markets: Evidence from the quantile VAR network, *J. Environ. Manage.*, **306** (2022), 114493. https://doi.org/10.1016/j.jenvman.2022.114493

13. S. Long, Z. Li, Dynamic spillover effects of global financial stress: Evidence from the quantile var network, *Int. Rev. Financ. Anal.*, **90** (2023), 102945. https://doi.org/10.1016/j.irfa.2023.102945

14. M. E. Hoque, M. Billah, B. Kapar, M. A. Naeem, Quantifying the volatility spillover dynamics between financial stress and us financial sectors: Evidence from QVAR connectedness, *Int. Rev. Financ. Anal.*, **95** (2024), 103434. https://doi.org/10.1016/j.irfa.2024.103434

15. J. Wang, S. Mishra, A. Sharif, H. Chen, Dynamic spillover connectedness among green finance and policy uncertainty: Evidence from QVAR network approach, *Energ. Econ.*, **131** (2024), 107330. https://doi.org/10.1016/j.eneco.2024.107330

16. N. Kyriazis, S. Papadamou, P. Tzeremes, S. Corbet, Examining spillovers and connectedness among commodities, inflation, and uncertainty: A quantile-VAR framework, *Energ. Econ.*, **133** (2024), 107508. https://doi.org/10.1016/j.eneco.2024.107330

17. D. J. Kim, E. Noh, S. Y. Choi, Quantile spillover effects and sector dynamics in US stock markets: Normal vs. extreme market conditions, *Financ. Res. Lett.*, **83** (2025), 107608. https://doi.org/10.1016/j.frl.2025.107608

18. F. Zhu, S. Fu, X. Liu, A quantile spillover-driven markov switching model for volatility forecasting: Evidence from the cryptocurrency market, *Mathematics*, **13** (2025), 2382. https://doi.org/10.3390/math13152382

19. J. Cunado, I. Chatziantoniou, D. Gabauer, F. P. de Gracia, M. Hardik, Dynamic spillovers across precious metals and oil realized volatilities: Evidence from quantile extended joint connectedness measures, *J. Commod. Mark.*, **30** (2023), 100327. https://doi.org/10.1016/j.jcomm.2023.100327

20. I. Chatziantoniou, D. Gabauer, H. A. Marfatia, Dynamic connectedness and spillovers across sectors: Evidence from the indian stock market, *Scot. J. Polit. Econ.*, **69** (2022), 283–300. https://doi.org/10.1111/sjpe.12291

21. R. Gupta, H. A. Marfatia, The impact of unconventional monetary policy shocks in the us on emerging market reits, *J. Real Estate Lit.*, **26** (2018), 175–188. https://doi.org/10.1080/10835547.2018.12090476

22. G. Bekaert, E. C. Engstrom, N. R. Xu, The time variation in risk appetite and uncertainty, *Manage. Sci.*, **68** (2022), 3975–4004. https://doi.org/10.1287/mnsc.2021.4068

23. I. Chatziantoniou, D. Gabauer, A. Stenfors, Interest rate swaps and the transmission mechanism of monetary policy: A quantile connectedness approach, *Econ. Lett.*, **204** (2021), 109891. https://doi.org/10.1016/j.econlet.2021.109891

24. I. Chatziantoniou, E. J. A. Abakah, D. Gabauer, A. K. Tiwari, Quantile time–frequency price connectedness between green bond, green equity, sustainable investments and clean energy markets, *J. Clean. Prod.*, **361** (2022), 132088. https://doi.org/10.1016/j.jclepro.2022.132088

25. E. Bouri, T. Saeed, X. V. Vo, D. Roubaud, Quantile connectedness in the cryptocurrency market, *J. Int. Financ. Mark. I.*, **71** (2021), 101302. https://doi.org/10.1016/j.intfin.2021.101302

26. M. Zhao, H. Park, Quantile time-frequency spillovers among green bonds, cryptocurrencies, and conventional financial markets, *Int. Rev. Financ. Anal.*, **93** (2024), 103198. https://doi.org/10.1016/j.irfa.2024.103198

27. P. Joshi, Regime-specific interdependencies in cryptocurrency markets: A high-frequency gmm-var approach, *Data Sci. Financ. Econ.*, **5** (2025), 419–439. https://doi.org/10.3934/DSFE.2025017

28. P. S. Ko, K. S. Chen, Discovering ai tokens in the fractal markets hypothesis and their time-frequency co-movements with the leading high-carbon cryptocurrency, *Data Sci. Financ. Econ.*, **5** (2025), 293–319. https://doi.org/10.3934/DSFE.2025013

29. M. Abdullah, D. Adeabah, E. J. A. Abakah, C. C. Lee, Extreme return and volatility connectedness among real estate tokens, REITs, and other assets: The role of global factors and portfolio implications, *Financ. Res. Lett.*, **56** (2023), 104062. https://doi.org/10.1016/j.frl.2023.104062

30. H. Asgharian, C. Christiansen, A. J. Hou, The effect of uncertainty on stock market volatility and correlation, *J. Bank. Financ.*, **154** (2023), 106929. https://doi.org/10.1016/j.jbankfin.2023.106929

31. C. Huber, J. Huber, M. Kirchler, Market shocks and professionals' investment behavior–evidence from the COVID-19 crash, *J. Bank. Financ.*, **133** (2021), 106247. https://doi.org/10.1016/j.jbankfin.2021.106247

32. V. Coudert, M. Gex, Does risk aversion drive financial crises? testing the predictive power of empirical indicators, *J. Empir. Financ.*, **15** (2008), 167–184. https://doi.org/10.1016/j.jempfin.2007.06.001

33. G. Bekaert, M. Hoerova, M. L. Duca, Risk, uncertainty and monetary policy, *J. Monetary Econ.*, **60** (2013), 771–788. https://doi.org/10.1016/j.jmoneco.2013.06.003

34. S. J. H. Shahzad, E. Bouri, D. Roubaud, L. Kristoufek, B. Lucey, Is bitcoin a better safe-haven investment than gold and commodities?, *Int. Rev. Financ. Anal.*, **63** (2019), 322–330. https://doi.org/10.1016/j.irfa.2019.01.002

35. L. A. Smales, Bitcoin as a safe haven: Is it even worth considering?, *Financ. Res. Lett.*, **30** (2019), 385–393. https://doi.org/10.1016/j.frl.2018.11.002

36. M. Umar, C. W. Su, S. K. A. Rizvi, X. F. Shao, Bitcoin: A safe haven asset and a winner amid political and economic uncertainties in the us?, *Technol. Forecast. Soc.*, **167** (2021), 120680. https://doi.org/10.1016/j.techfore.2021.120680

37. E. Bouri, P. Molnár, G. Azzi, D. Roubaud, L. I. Hagfors, On the hedge and safe haven properties of bitcoin: Is it really more than a diversifier?, *Financ. Res. Lett.*, **20** (2017), 192–198. https://doi.org/10.1016/j.frl.2016.09.025

38. A. Kliber, P. Marszałek, I. Musiałkowska, K. Świerczyńska, Bitcoin: Safe haven, hedge or diversifier? Perception of Bitcoin in the context of a country's economic situation—a stochastic volatility approach, *Physica A*, **524** (2019), 246–257. https://doi.org/10.1016/j.physa.2019.04.145

39. E. Bouri, S. J. H. Shahzad, D. Roubaud, L. Kristoufek, B. Lucey, Bitcoin, gold, and commodities as safe havens for stocks: New insight through wavelet analysis, *Q. Rev. Econ. Financ.*, **77** (2020), 156–164. https://doi.org/10.1016/j.qref.2020.03.004

40. S. J. H. Shahzad, E. Bouri, D. Roubaud, L. Kristoufek, Safe haven, hedge and diversification for G7 stock markets: Gold versus Bitcoin, *Econ. Model.*, **87** (2020), 212–224. https://doi.org/10.5325/pennhistory.87.1.0212

41. D. G. Baur, B. M. Lucey, Is gold a hedge or a safe haven? An analysis of stocks, bonds and gold, *Financ. Rev.*, **45** (2010), 217–229. https://doi.org/10.1111/j.1540-6288.2010.00244.x

42. N. Antonakakis, I. Chatziantoniou, D. Gabauer, Refined measures of dynamic connectedness based on time-varying parameter vector autoregressions, *J. Risk Financ. Manag.*, **13** (2020), 84. https://doi.org/10.3390/jrfm13040084

43. T. Ando, M. Greenwood-Nimmo, Y. Shin, Quantile connectedness: Modeling tail behavior in the topology of financial networks, *Manage. Sci.*, **68** (2022), 2401–2431. https://doi.org/10.1287/mnsc.2021.3984

44. S. Corbet, Y. Hou, Y. Hu, L. Oxley, Time varying risk aversion and its connectedness: Evidence from cryptocurrencies, *Ann. Oper. Res.*, **338** (2024), 879–923. https://doi.org/10.1007/s10479-024-06001-9

45. R. Demirer, K. Gkillas, R. Gupta, C. Pierdzioch, Risk aversion and the predictability of crude oil market volatility: A forecasting experiment with random forests, *J. Oper. Res. Soc.*, **73** (2022), 1755–1767. https://doi.org/10.1080/01605682.2021.1936668

46. C. Pflueger, G. Rinaldi, Why does the fed move markets so much? A model of monetary policy and time-varying risk aversion, *J. Financ. Econ.*, **146** (2022), 71–89. https://doi.org/10.1016/j.jfineco.2022.06.002

47. X. Wu, Q. He, H. Xie, Forecasting VIX with time-varying risk aversion, *Int. Rev. Econ. Financ.*, **88** (2023), 458–475. https://doi.org/10.1016/j.iref.2023.06.034

48. Z. Umar, A. Bossman, T. Teplova, E. Marfo-Yiadom, Does time-varying risk aversion sentiment matter in the connectedness among Sub-Saharan African bond markets?, *Emerg. Mark. Rev.*, **61** (2024), 101160. https://doi.org/10.1016/j.ememar.2024.101160

49. S. Y. Choi, E. Hadad, The dynamic relationship among economic and monetary policy, geopolitical risk, sentiment, and risk aversion: A TVP-VAR approach, *Financ. Res. Lett.*, **72** (2025), 106532. https://doi.org/10.1016/j.frl.2024.106532

50. A. Sokhanvar, S. Hammoudeh, Comparative analysis of responses of risky and safe haven assets to stock market risk before and after the yield curve inversions in the US, *Int. Rev. Econ. Financ.*, **94** (2024), 103376. https://doi.org/10.1016/j.iref.2024.103376

51. T. C. Chiang, Can gold or silver be used as a hedge against policy uncertainty and COVID-19 in the Chinese market?, *China Financ. Rev. Int.*, **12** (2022), 571–600. https://doi.org/10.1108/CFRI-12-2021-0232

52. D. G. Baur, L. A. Smales, Hedging geopolitical risk with precious metals, *J. Bank. Financ.*, **117** (2020), 105823. https://doi.org/10.1016/j.jbankfin.2020.105823

53. B. Elie, J. Naji, A. Dutta, G. S. Uddin, Gold and crude oil as safe-haven assets for clean energy stock indices: Blended copulas approach, *Energy*, **178** (2019), 544–553. https://doi.org/10.1016/j.energy.2019.04.155

54. S. Skapa, Commodities as a tool of risk diversification, *Equilibrium*, **8** (2013), 65–77. https://doi.org/10.12775/EQUIL.2013.014

55. B. Li, Speculation, risk aversion, and risk premiums in the crude oil market, *J. Bank. Financ.*, **95** (2018), 64–81. https://doi.org/10.1016/j.jbankfin.2018.06.002

56. N. A. Kyriazis, S. Papadamou, P. Tzeremes, Are benchmark stock indices, precious metals or cryptocurrencies efficient hedges against crises?, *Econ. Model.*, **128** (2023), 106502. https://doi.org/10.1016/j.econmod.2023.106502

57. R. M. Dias, M. Chambino, N. Teixeira, P. Alexandre, P. Heliodoro, Balancing portfolios with metals: A safe haven for green energy investors?, *Energies*, **16** (2023), 7197. https://doi.org/10.3390/en16207197

58. S. W. Kim, B. S. Lee, Stock returns, asymmetric volatility, risk aversion, and business cycle: Some new evidence, *Econ. Inq.*, **46** (2008), 131–148. https://doi.org/10.1111/j.1465-7295.2007.00066.x

59. B. J. Cohen, The yuan tomorrow? Evaluating China's currency internationalisation strategy, *New Polit. Econ.*, **17** (2012), 361–371. https://doi.org/10.1080/13563467.2011.615915

60. R. J. Caballero, E. Farhi, P. O. Gourinchas, The safe assets shortage conundrum, *J. Econ. Perspect.*, **31** (2017), 29–46. https://doi.org/10.1257/jep.31.3.29

61. L. Peritz, R. Weldzius, R. Rogowski, T. Flaherty, Enduring the great recession: Economic integration in the European union, *Rev. Int. Organ.*, **17** (2022), 175–203. https://doi.org/10.1007/s11558-020-09410-0

62. C. Jin, X. Tian, Enhanced safe-haven status of Bitcoin: Evidence from the silicon valley bank collapse, *Financ. Res. Lett.*, **59** (2024), 104689. https://doi.org/10.1016/j.frl.2023.104689

63. K. J. Lansing, S. F. LeRoy, Risk aversion, investor information and stock market volatility, *Eur. Econ. Rev.*, **70** (2014), 88–107. https://doi.org/10.1016/j.euroecorev.2014.03.009

64. D. A. Guenther, R. Sansing, The effect of tax-exempt investors and risk on stock ownership and expected returns, *Account. Rev.*, **85** (2010), 849–875. https://doi.org/10.2308/accr.2010.85.3.849

65. C. Wu, C. H. Yu, Risk aversion and the yield of corporate debt, *J. Bank. Financ.*, **20** (1996), 267–281. https://doi.org/10.1016/0378-4266(94)00099-9

66. J. L. Glascock, D. Michayluk, K. Neuhauser, The riskiness of REITs surrounding the October 1997 stock market decline, *J. Real Estate Financ.*, **28** (2004), 339–354. https://doi.org/10.1023/B:REAL.0000018786.39272.fa

67. R. Demirer, A. Yüksel, A. Yüksel, On the hedging benefits of reits: The role of risk aversion and market states, *Econ. Bus. Lett.*, **10** (2021), 126–132. https://doi.org/10.17811/ebl.10.2.2021.126-132

68. J. Y. Campbell, J. H. Cochrane, By force of habit: A consumption-based explanation of aggregate stock market behavior, *J. Polit. Econ.*, **107** (1999), 205–251. https://doi.org/10.1086/250059

69. M. K. Brunnermeier, L. H. Pedersen, Market liquidity and funding liquidity, *Rev. Financ. Stud.*, **22** (2009), 2201–2238. https://doi.org/10.1093/rfs/hhn098

70. R. J. Caballero, A. Krishnamurthy, Collective risk management in a flight to quality episode, *J. Financ.*, **63** (2008), 2195–2230. https://doi.org/10.1111/j.1540-6261.2008.01394.x

71. D. G. Baur, K. Hong, A. D. Lee, Bitcoin: Medium of exchange or speculative assets?, *J. Int. Financ. Mark. I.*, **54** (2018), 177–189. https://doi.org/10.1016/j.intfin.2017.12.004

72. S. Choi, J. Shin, Bitcoin: An inflation hedge but not a safe haven, *Financ. Res. Lett.*, **46** (2022), 102379. https://doi.org/10.1016/j.frl.2021.102379

73. G. Koop, M. H. Pesaran, S. M. Potter, Impulse response analysis in nonlinear multivariate models, *J. Econometrics*, **74** (1996), 119–147. https://doi.org/10.1016/0304-4076(95)01753-4

74. H. H. Pesaran, Y. Shin, Generalized impulse response analysis in linear multivariate models, *Econ. Lett.*, **58** (1998), 17–29. https://doi.org/10.1016/S0165-1765(97)00214-0

75. F. X. Diebold, K. Yilmaz, Better to give than to receive: Predictive directional measurement of volatility spillovers, *Int. J. Forecast.*, **28** (2012), 57–66. https://doi.org/10.1016/j.ijforecast.2011.02.006

76. R. Koenker, G. Bassett Jr, Regression quantiles, *Econometrica*, **46** (1978), 33–50. https://doi.org/10.2307/1913643

77. M. K. Brunnermeier, L. H. Pedersen, Market liquidity and funding liquidity, *Rev. Financ. Stud.*, **22** (2009), 2201–2238. https://doi.org/10.1093/rfs/hhn098

78. J. B. Kim, L. Luo, H. Xie, Do dividends mitigate bad news hoarding, overinvestments, and stock price crash risk?, *Account. Financ.*, **64** (2024), 3999–4038. https://doi.org/10.1111/acfi.13297

79. A. Belanes, F. Saâdaoui, A. Amirat, H. Rabbouch, Safety assessment of cryptocurrencies as risky assets during the COVID-19 pandemic, *Physica A*, **651** (2024), 130013. https://doi.org/10.1016/j.physa.2024.130013

80. M. Qadan, D. Kliger, N. Chen, Idiosyncratic volatility, the vix and stock returns, *N. Am. J. Econ. Financ.*, **47** (2019), 431–441. https://doi.org/10.1016/j.najef.2018.06.003

81. D. Bams, I. Honarvar, Vix and liquidity premium, *Int. Rev. Financ. Anal.*, **74** (2021), 101655. https://doi.org/10.1016/j.irfa.2020.101655

82. A. H. Elsayed, G. Gozgor, C. K. M. Lau, Risk transmissions between Bitcoin and traditional financial assets during the COVID-19 era: The role of global uncertainties, *Int. Rev. Financ. Anal.*, **81** (2022), 102069. https://doi.org/10.1016/j.irfa.2022.102069

83. B. Gaies, N. Chaâbane, N. Arfaoui, J. M. Sahut, On the resilience of cryptocurrencies: A quantile-frequency analysis of Bitcoin and ethereum reactions in times of inflation and financial instability, *Res. Int. Bus. Financ.*, **70** (2024), 102302. https://doi.org/10.1016/j.ribaf.2024.102302

84. J. Annaert, M. De Ceuster, P. V. Roy, C. Vespro, What determines Euro area bank CDS spreads?, *J. Int. Money Financ.*, **32** (2013), 444–461. https://doi.org/10.1016/j.jimonfin.2012.05.029

85. T. Leung, R. Sircar, T. Zariphopoulou, *Credit derivatives and risk aversion*, In: Econometrics and Risk Management, Emerald Group Publishing Limited, 2008, 275–291. https://doi.org/10.1016/S0731-9053(08)22011-6

86. A. M'beirick, S. Haddou, The asymmetric response of sovereign credit default swaps spreads to risk aversion, investor sentiment and monetary policy shocks, *Int. Rev. Econ. Financ.*, **93** (2024), 244–272. https://doi.org/10.1016/j.iref.2024.03.064

87. J. Yu, Y. Yuan, Investor sentiment and the mean-variance relation, *J. Financ. Econ.*, **100** (2011), 367–381. https://doi.org/10.1016/j.jfineco.2010.10.011

88. A. Bandopadhyaya, A. L. Jones, *Measuring investor sentiment in equity markets*, In: Asset Management: Portfolio Construction, Performance and Returns, Springer, 2016, 258–269. https://doi.org/10.1007/978-3-319-30794-7_11

89. S. N. Ung, B. Gebka, R. D. Anderson, An enhanced investor sentiment index, *Eur. J. Financ.*, **30** (2024), 827–864. https://doi.org/10.1080/1351847X.2023.2247440

AIMS Press